I Raggi Cosmici di Ultra Alta Energia

Corso di **Fisica Astroparticellare**

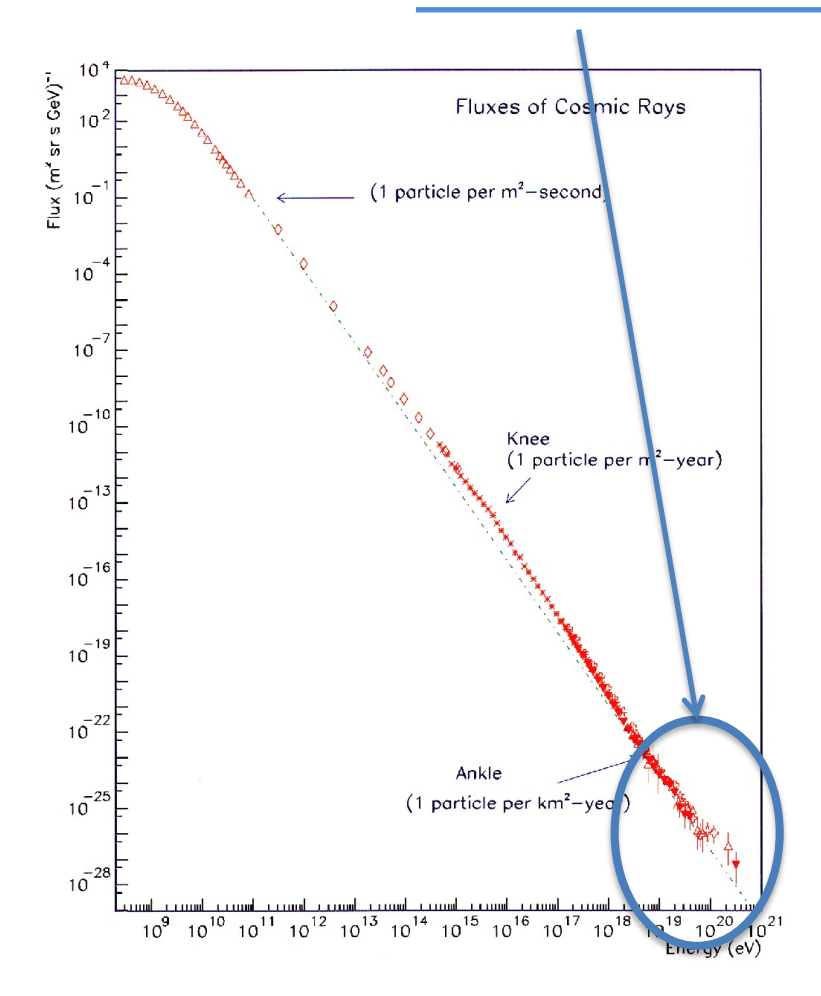
Lino Miramonti



Testi consigliati (su cui si basano queste lezioni):

- Alessandro De Angelis, Mário João Martins Pimenta Introduction to Particle and Astroparticle Physics (Springer 2015, Springer 2018)
- Maurizio Spurio Particles and Astrophysics (Springer 2014)
- Maurizio Spurio The Probes of Multimessanger Astrophysics (Springer 2018)
- Claus Grupen Astroparticle Physics (Springer 2005, Springer 2020)

UHECRs: CRs with E> 10¹⁸ eV



Nearly uniform **power-law spectrum E**-γ:

- 10 orders of magnitude in Energy
- 32 orders of magnitude in flux

OPEN QUESTIONS:

<u>Where</u> and <u>how</u> these cosmic rays are accelerated to these energies

Which are the <u>sources</u> that generated these cosmic rays

The chemical composition is unknown

From a Particle Physics point of view:

UHE Cosmic Rays probe physics at energies out of reach of any man made accelerator

LHC 14 TeV (cms) UHECRs
400 TeV (cms)

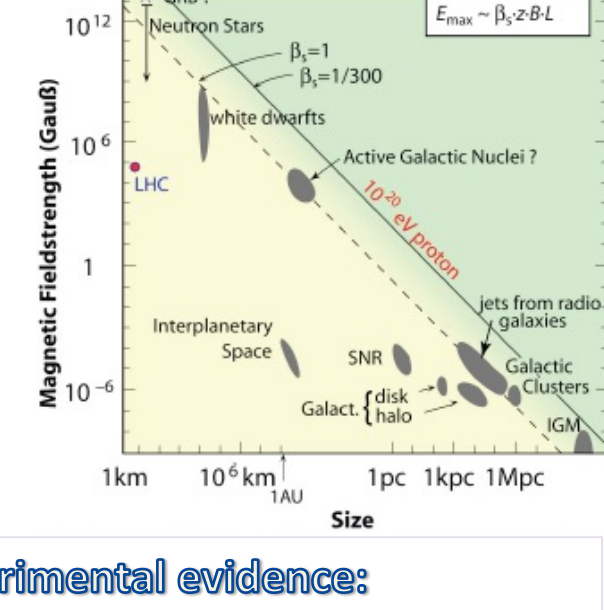


Possible UHECR Sources: 2 scenarios

Bottom-Up Acceleration

(Astrophysical Acceleration Mechanisms)

UHECR's are accelerated in extended objects or catastrophic events (supernova remnants, rotating neutron stars, AGNs, radio galaxies)



Experimental evidence:

- ✓ anisotropy in arrival directions
- ✓ Photons < ≈1%

Top-Down Decay

(Physics Beyond the Standard Model)

photon flux with the PAO from the measurement o Decay of topological defects **Monopoles Relics** Supersymmetric particles Strongly interacting neutrinos Decay of massive new long lived particles Etc.

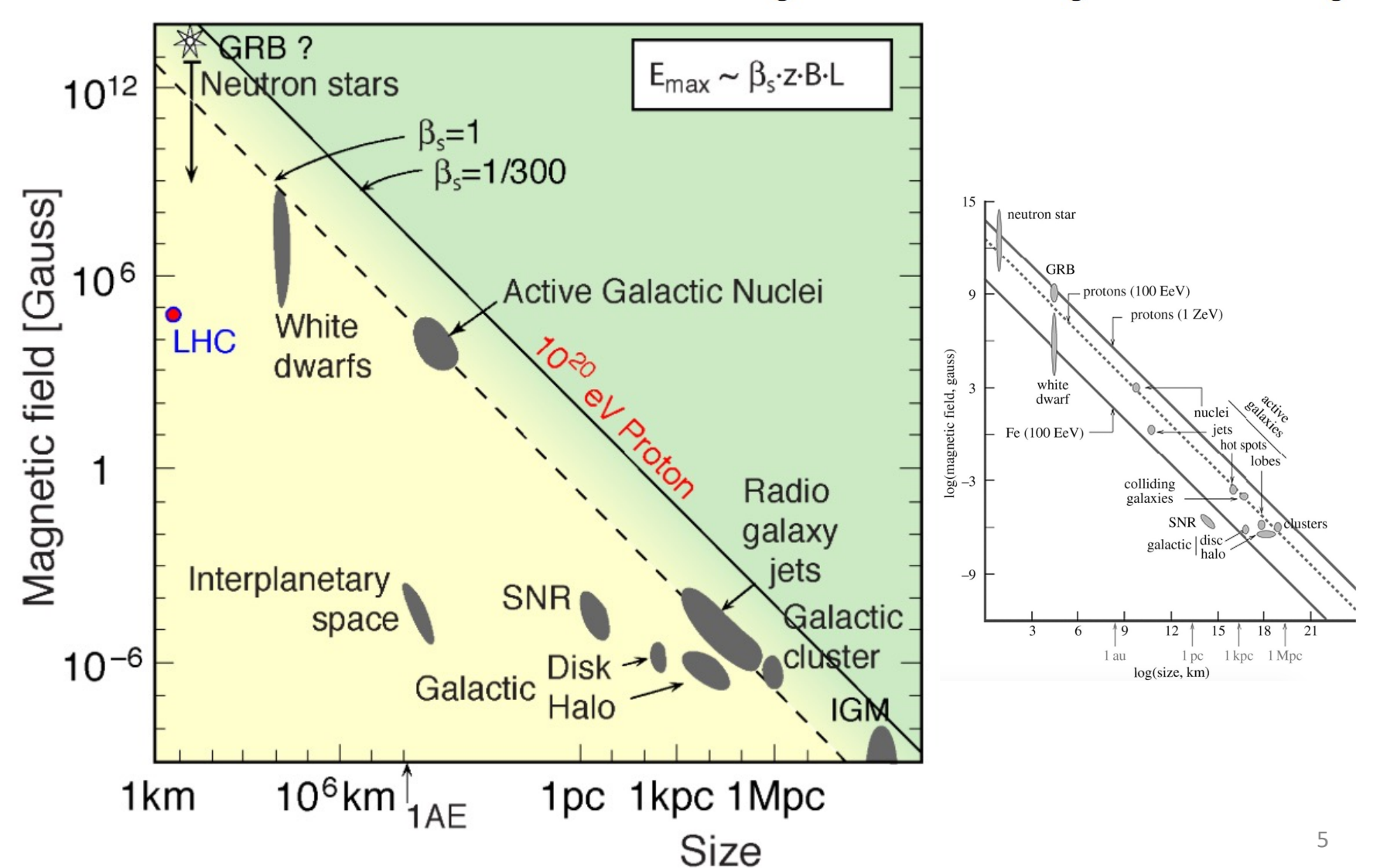
Experimental evidence:

- isotropy in arrival directions
- Photons $> \approx 10\%$

Hillas Plot (1984)

$$E_{max} \simeq 10^{18} \text{eV } Z \beta \left(\frac{R}{\text{kpc}}\right) \left(\frac{B}{\mu \text{G}}\right)$$

where β is the shock velocity, R is the size of the region and B the magnetic field strength.

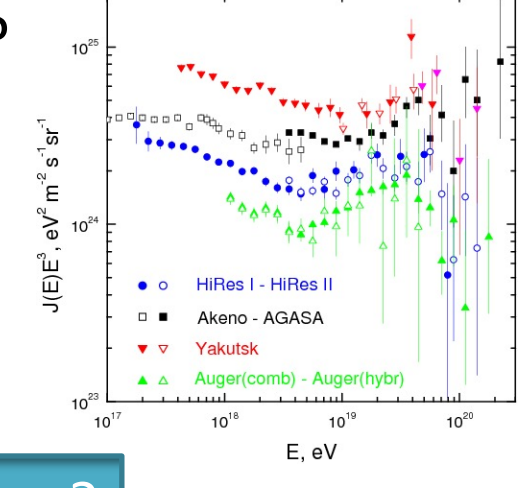


End to the cosmic ray spectrum?

Before AUGER it wasn't know if there were an end to the CR spectrum or not.

Now, we know (see later) that there is a suppression but we do not know its nature.

The suppression may be due to:



 $\propto Z B L$

propagation scenario

the interaction with Cosmic Microwave Background (CBM)

$$p + \gamma_{CMB} \rightarrow \Delta^{+} \rightarrow \pi + p / n \qquad E_{Th} \approx 6 \cdot 10^{19} \, eV$$

$$p + \gamma_{CMB} \rightarrow p + e^{+} + e^{-} \qquad E_{Th} \approx 5 \cdot 10^{17} \, eV$$

$$nuclei \qquad \text{(photodisintegration and pair production losses)}$$

$$A + \gamma_{CMB} \rightarrow (A - X) + X \qquad E_{Th} \approx Ax \, 1.5 \cdot 10^{19} \, eV$$

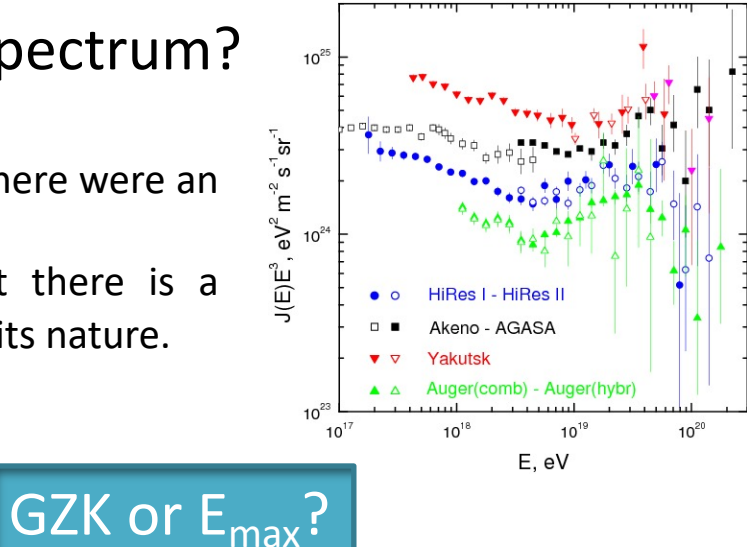
as forseen by Greisen, Zatsepin, Kuzmin in 1966 (the GZK cutoff)

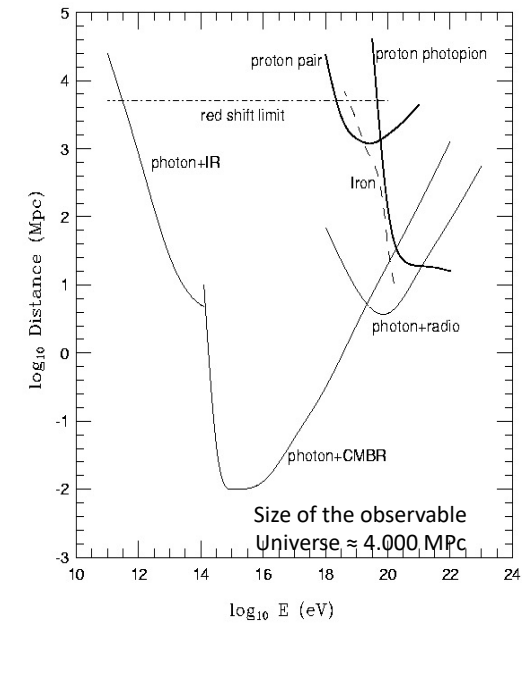
The **Universe is opaque** for protons with energy $> 6 \cdot 10^{19} \text{ eV}$ "horizon" (p and nuclei) ≈ 100 Mpc ($\approx 10^{20}$ eV)

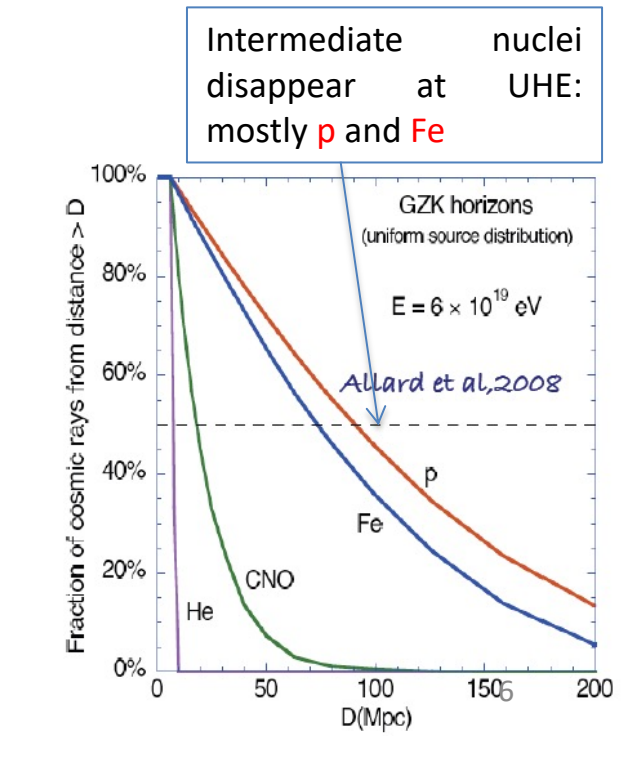
source scenario

to the reach of the maximum energy in the celestial accelerators:

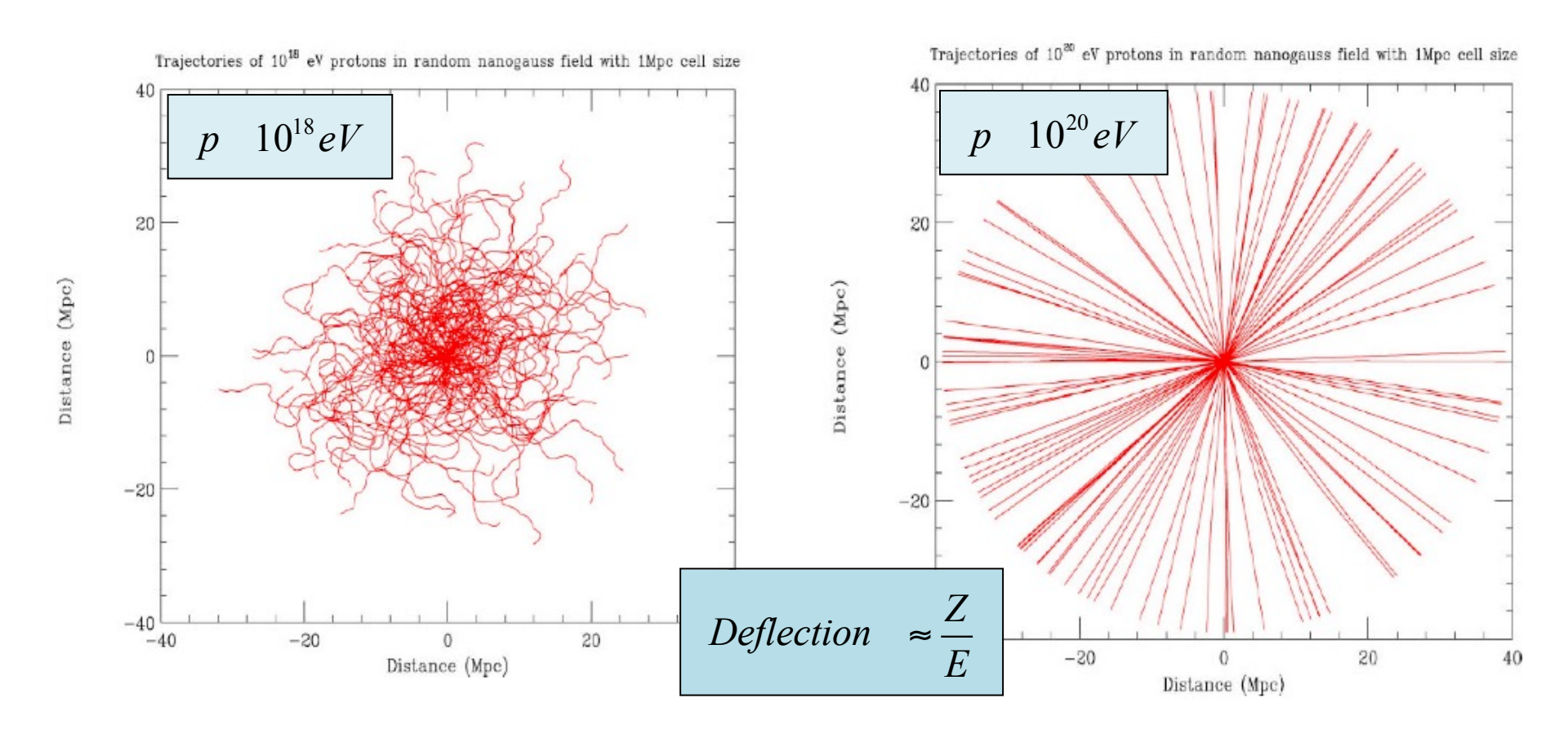
"source exhaustion" (i.e. maximum injection energy)







Influence of the Magnetic Field on propagation



Above 10^{20} eV $\Delta \phi < 2^{\circ}$ that is larger than the experimental resolution!

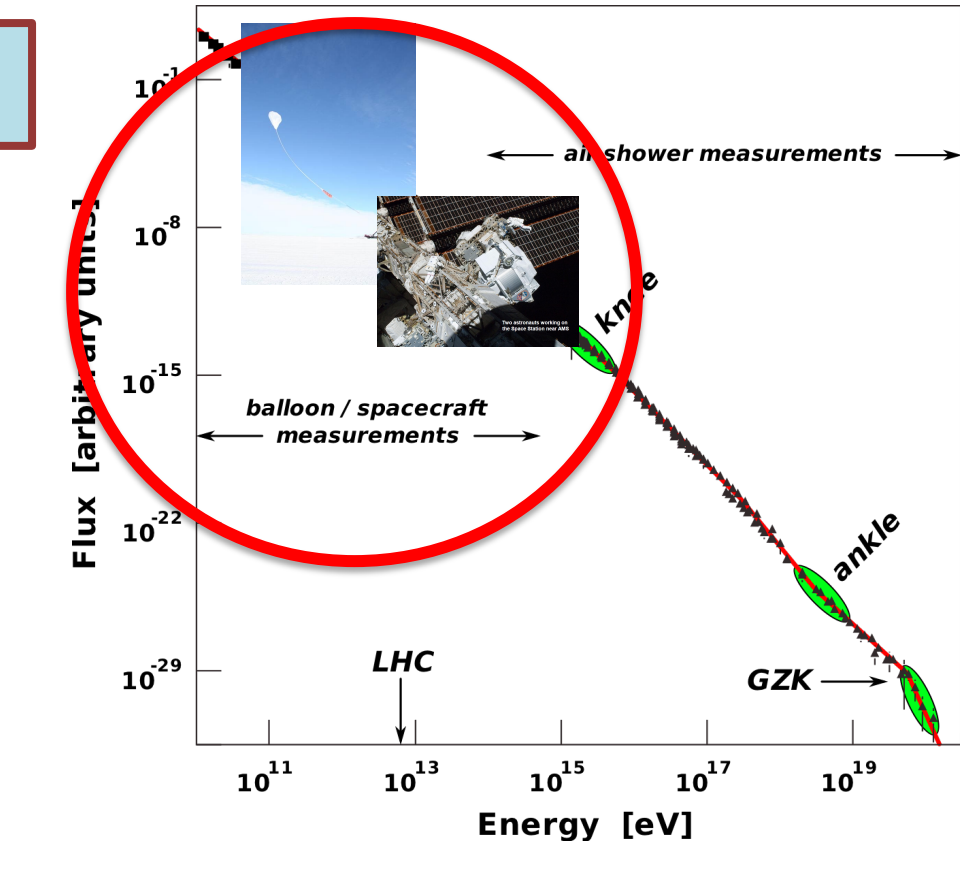
A window to Cosmic Rays Astronomy?

How to detect UHE-Cosmic Rays?

How to detect "low" CRs?

from **10**⁹ **eV** to **10**¹⁴ **eV**

 Up to 10¹⁴ eV it is possible to detect CR <u>directly</u> putting detectors on balloons or satellites



Energy measurement:

Simultaneous measurements of energy, charge, and mass (E, Z, A)

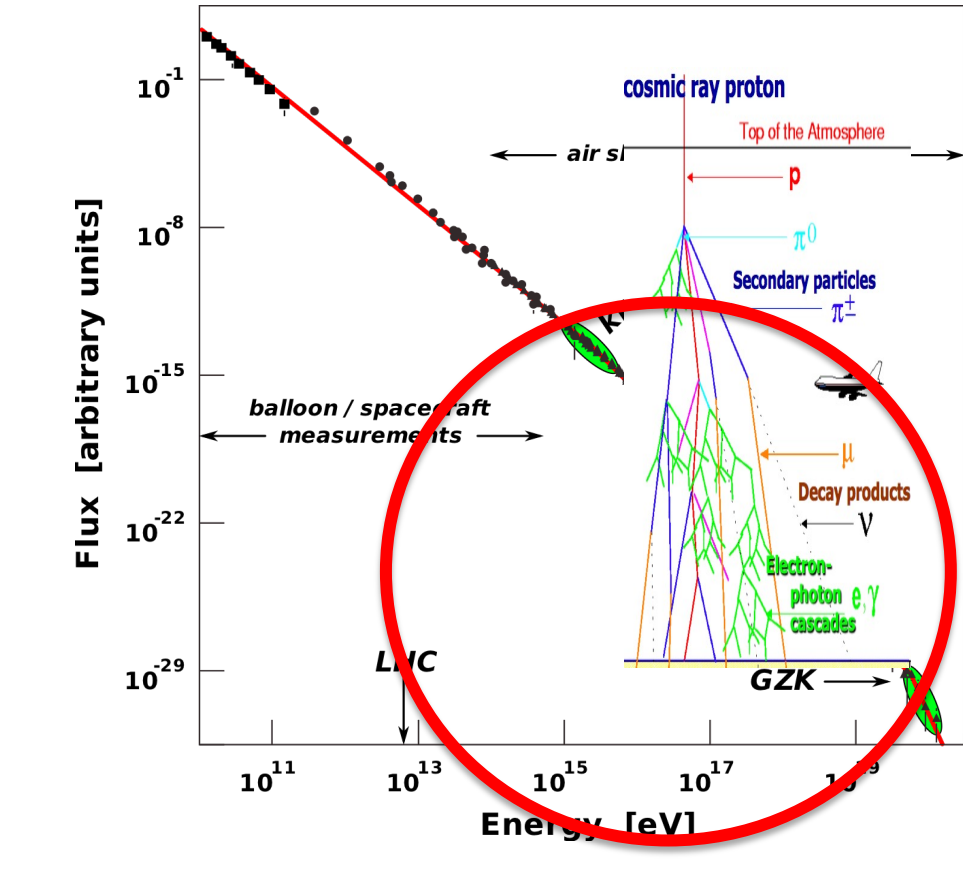
- From ~1 GeV to ~1 TeV magnetic spectrometers or Cherenkov detectors. (Individual elements are identified, characterized by their charge Z through the dE/dx method)
- At high energy Transition Radiation Detectors (TRDs)

The weight of a detector with a thickness of one hadronic interaction length and area of 1 m² amounts to \sim 1 ton.

How to detect CRs with E>10¹⁴ eV?

from **10**¹⁴ eV

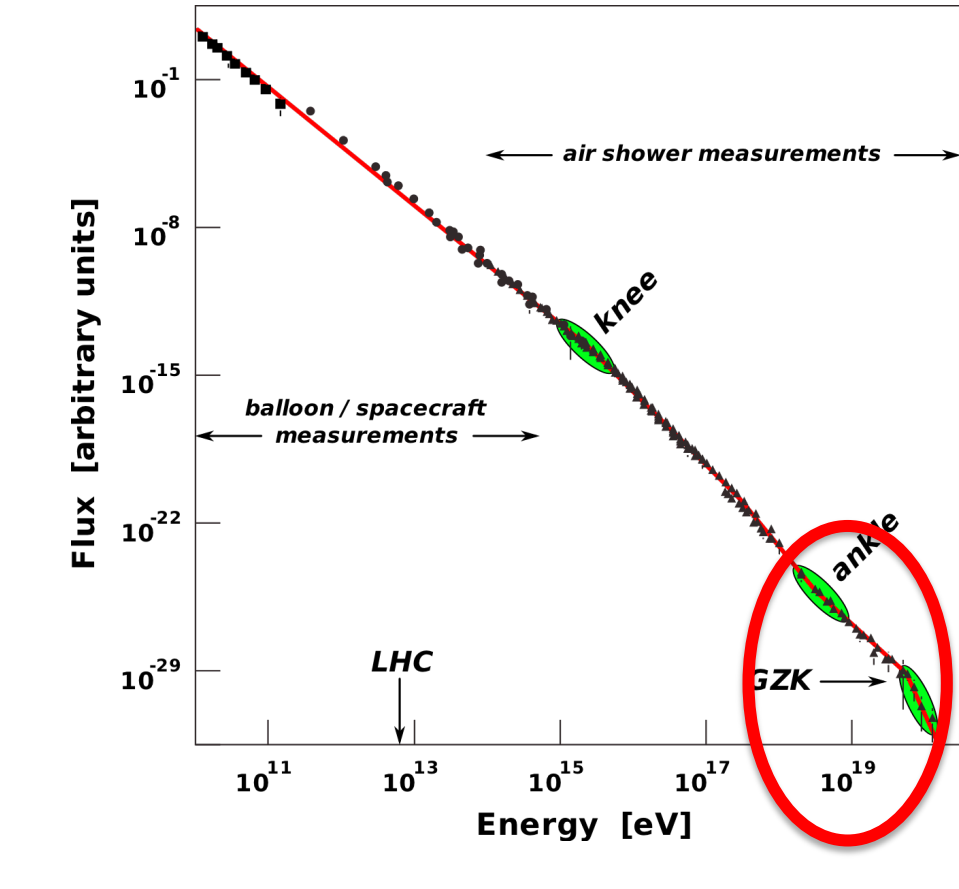
• For higher energy the flux is too poor and we have to study the showers (EAS) generated by primary CRs



How to detect UHECRs?

from 10¹⁸ eV

Showers (EAS) generated by Ultra High Energy CR (>10¹⁸ eV) are also studied detecting fluorescence light.



There are **two main techniques** to detect EAS from UHECRs:

- A) To sample the EAS at ground with an Array of surface detectors (Lateral profile)
- B) To detect the fluorescence light with Fluorescence telescopes (Longitudinal profile)

Array of surface detectors (Lateral profile)

The Surface Detector arrays samples the EAS at ground

- Time of arrival at each station

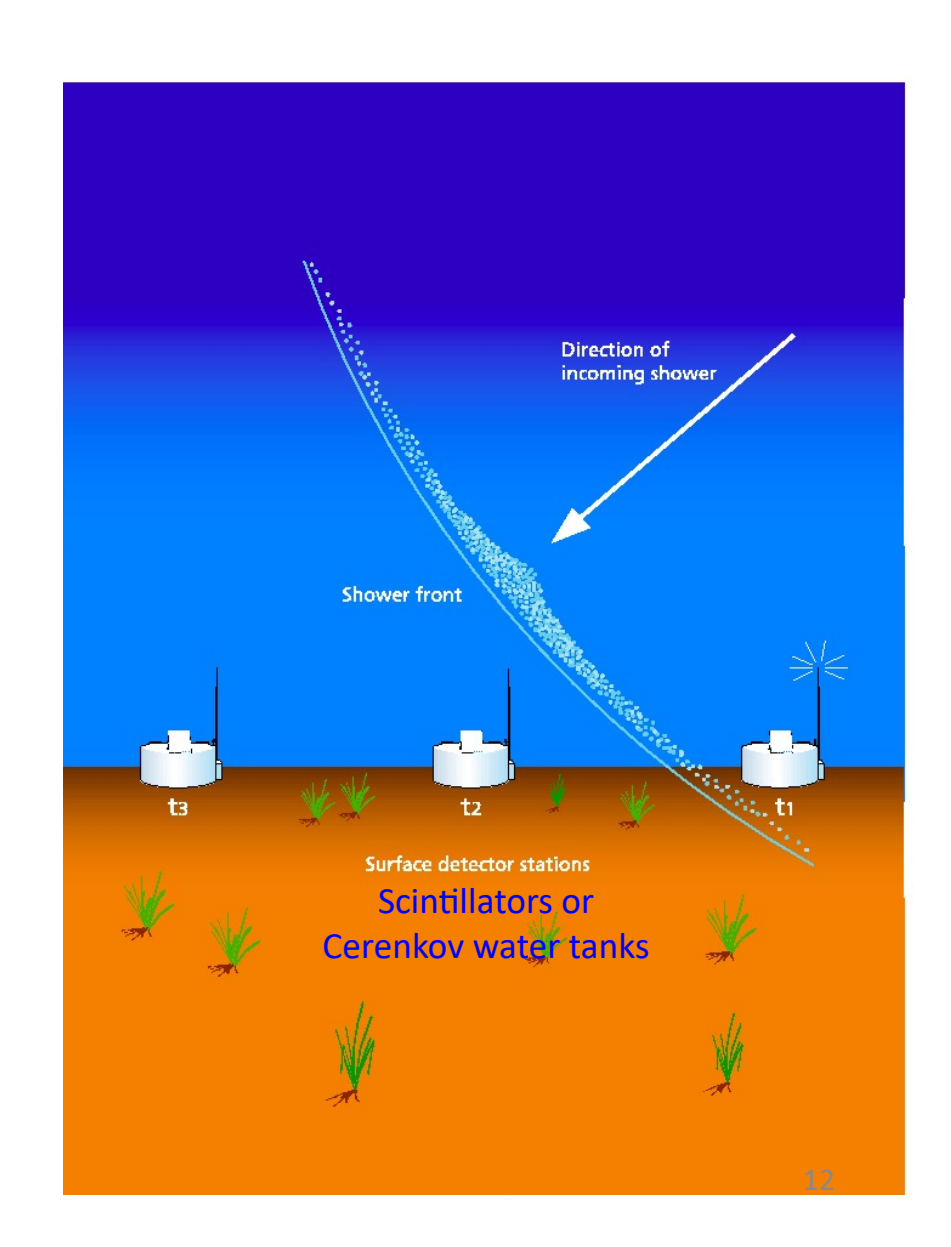
Thanks to the time of arrival it is possible to deduce the <u>arrival direction</u> of primary cosmic ray.

- Number of particles

From the number of secondary particles it is possible to infer the **energy** of primary cosmic ray.

- Muon number and Pulse rise time

Thanks to the number of muons and the study of the pulse rise time it is possible to measure the **mass** of primary cosmic ray.



Fluorescence telescopes (Longitudinal profile)

Secondary charged particles excite nitrogen molecules. The de-excitation process occurs in the UV (fluorescence)

M. Ave et al., Astropart. Phys. 28 (2007) 41

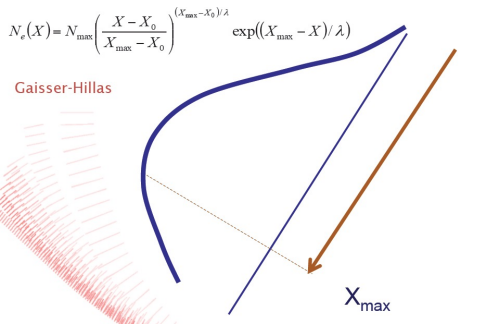
M. Ave et al., Astropart. Phys. 28 (2007) 41

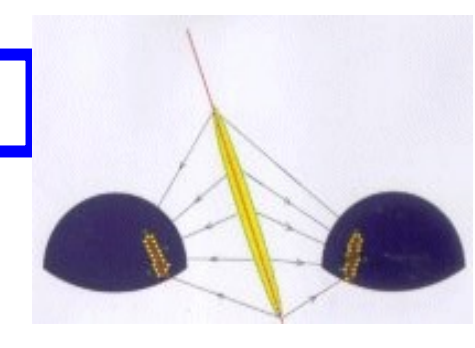
AIRFLY spectrum

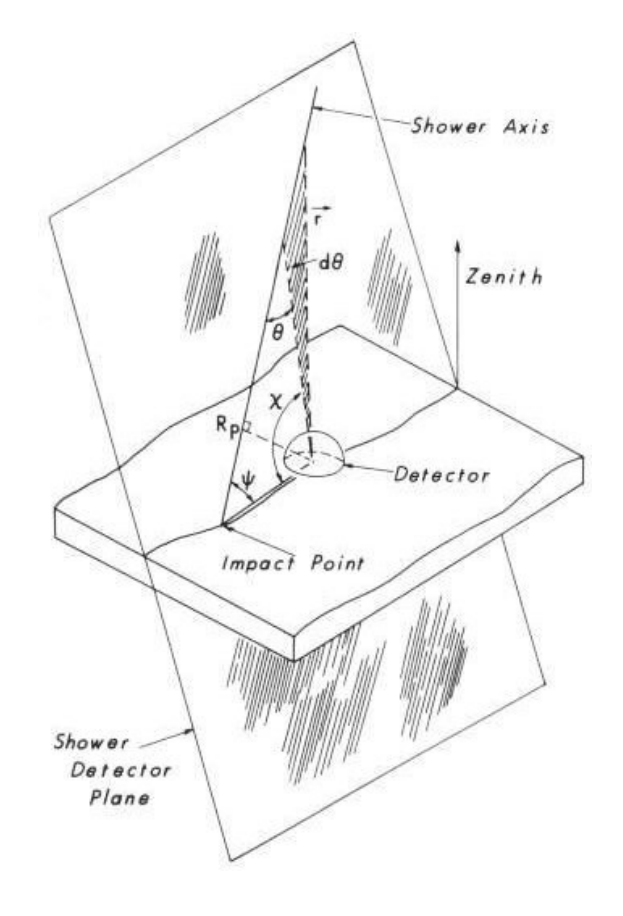
290 300 310 320 330 340 350 360 370 380 390 400 410 420

Wavelength (nm)

The fluorescence technique allows to measure the ionization density of the EAS at different altitudes. This enables to detect the longitudinal development of the shower.







Pros and Cons of two techniques

Array of surface detectors

Pros Duty cycle almost 100%

Cons Very strong dependence of nuclear interaction models (MonteCarlo simulations). Thus a big incertitude on the determination of the primary cosmic ray energy.

Fluorescence telescopes

Pros Less model dependent

Cons Duty cycle of about 10-15 % (clear moonless nights)

The Pierre Auger Observatory is an Hybrid detector that combines the two techniques.

Akeno Giant Air Shower Array operated in 1991~2004

▲TB45 **▲**TB44 MB\$NB44 TB46 STB43 NB46 NB4 TB47 TB36 TB16 NB27 AB41 TB35 TB41 TB15TB14 NB25 NB11 TB3 TB3 TB21 TB1/B12 △NB37 → NB21 → TB25 B22 → TB18 → TB25 B18 **△NB33** NB23 **△TB34** MB35 NB16 NB15 **SB29**

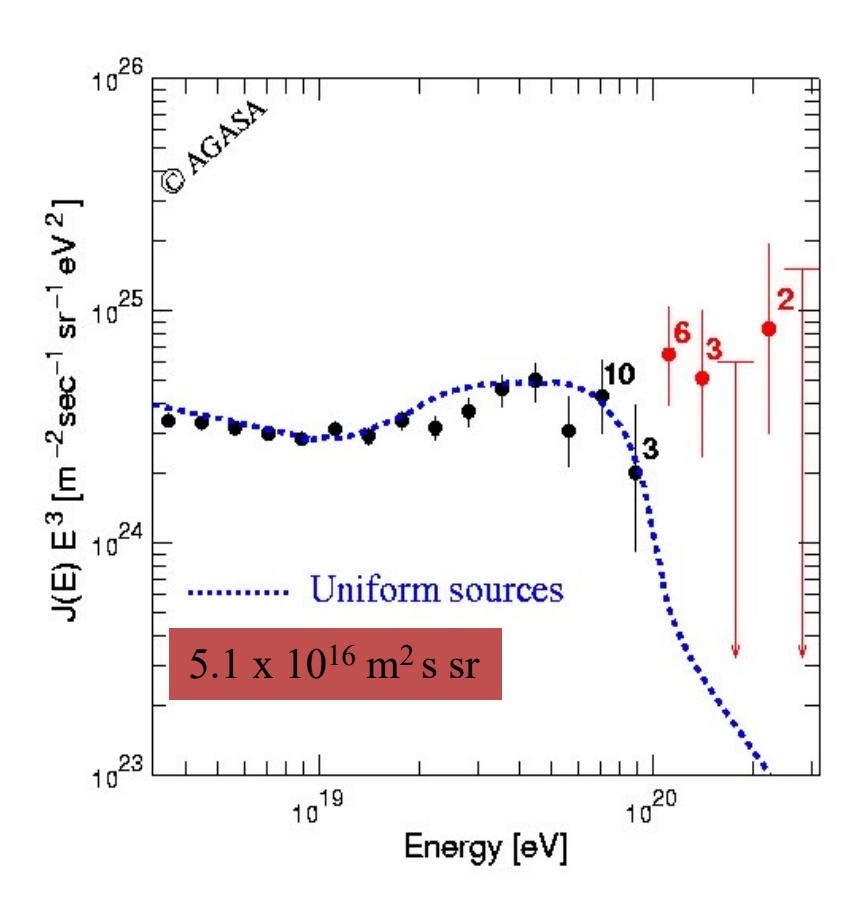
It covers an area of 100 km² and consists of

111 surface detectors and

27 muon detectors.



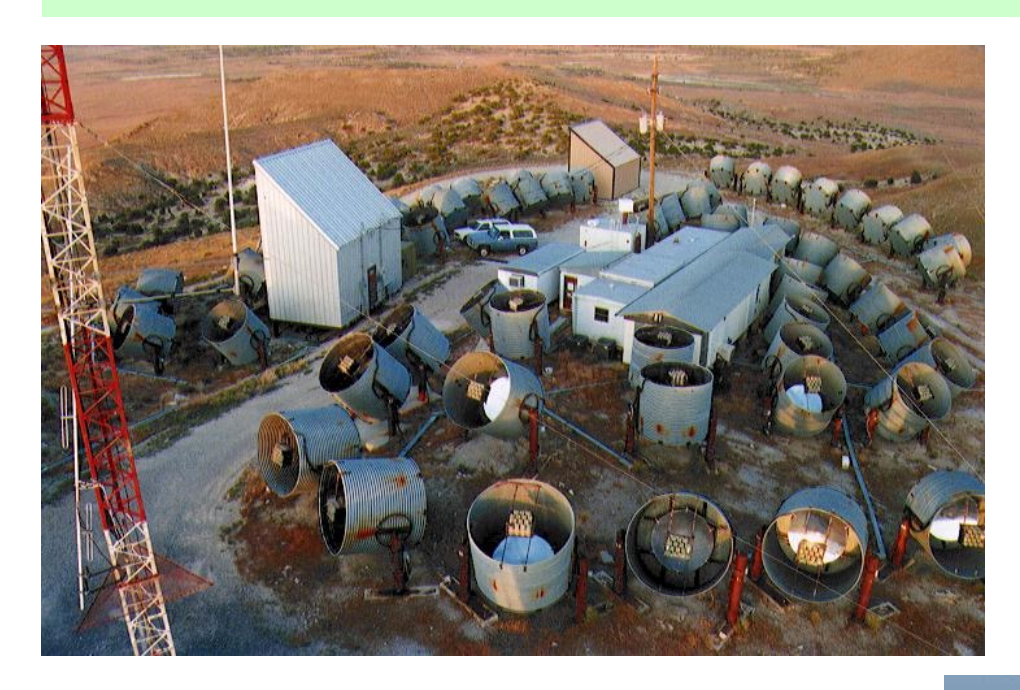
Energy Spectrum by AGASA (θ<45)

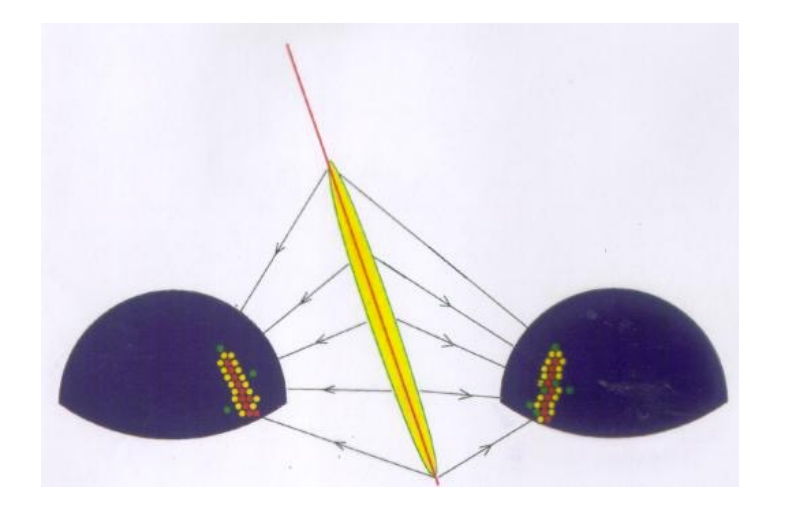


Super GZK particles

- Preliminary study with recent CORSIKA
 - If we evaluate energies with the recent CORSIKA
 - Energy scale shift down by ~10% at 10¹⁹eV and by ~15% at 10²⁰eV
 - 11 events above 10²⁰eV /
 1.3~2.6 expected
 → 5~6 events / 1.0~1.9 expected
- Small scale anisotropy of UHECR
 - The arrival direction of UHECRs is uniform in large scale
 - But AGASA data shows clusters, 1 triplets and 6 doublets → granularity
 - Source density ~10⁻⁵/Mpc³ ~ density of AGNs

The Fly's Eye Observatory (1981-1993)





The High Resolution Fly's Eye (**HiRes**)



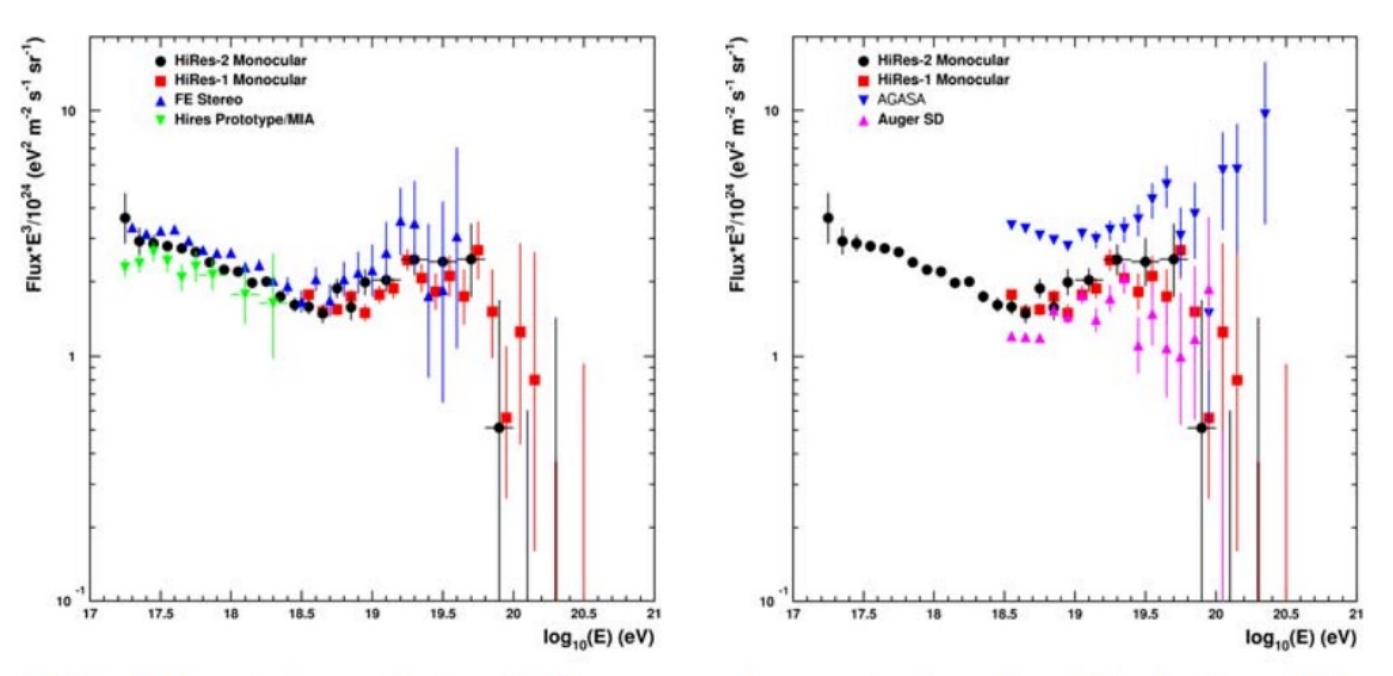
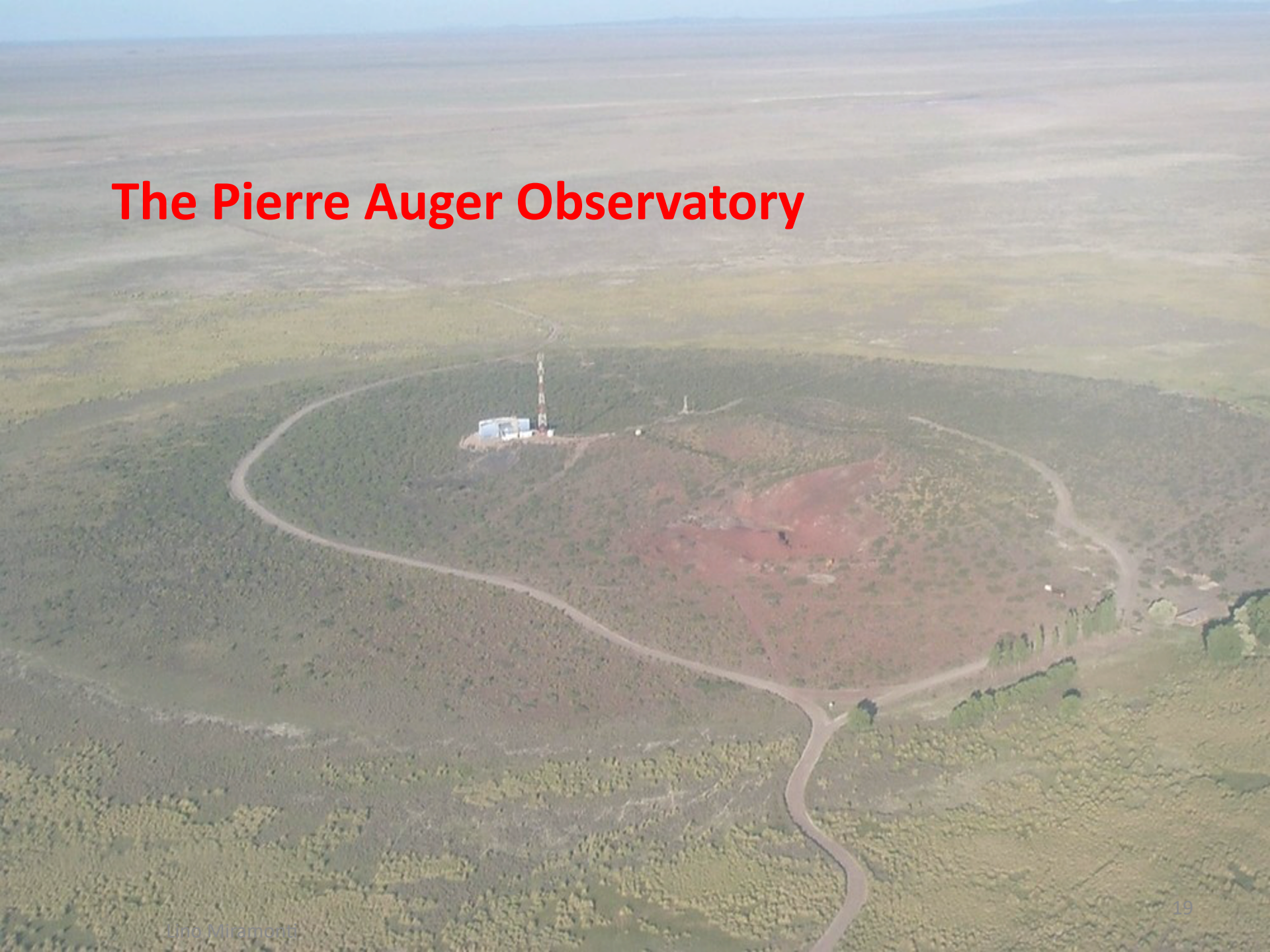
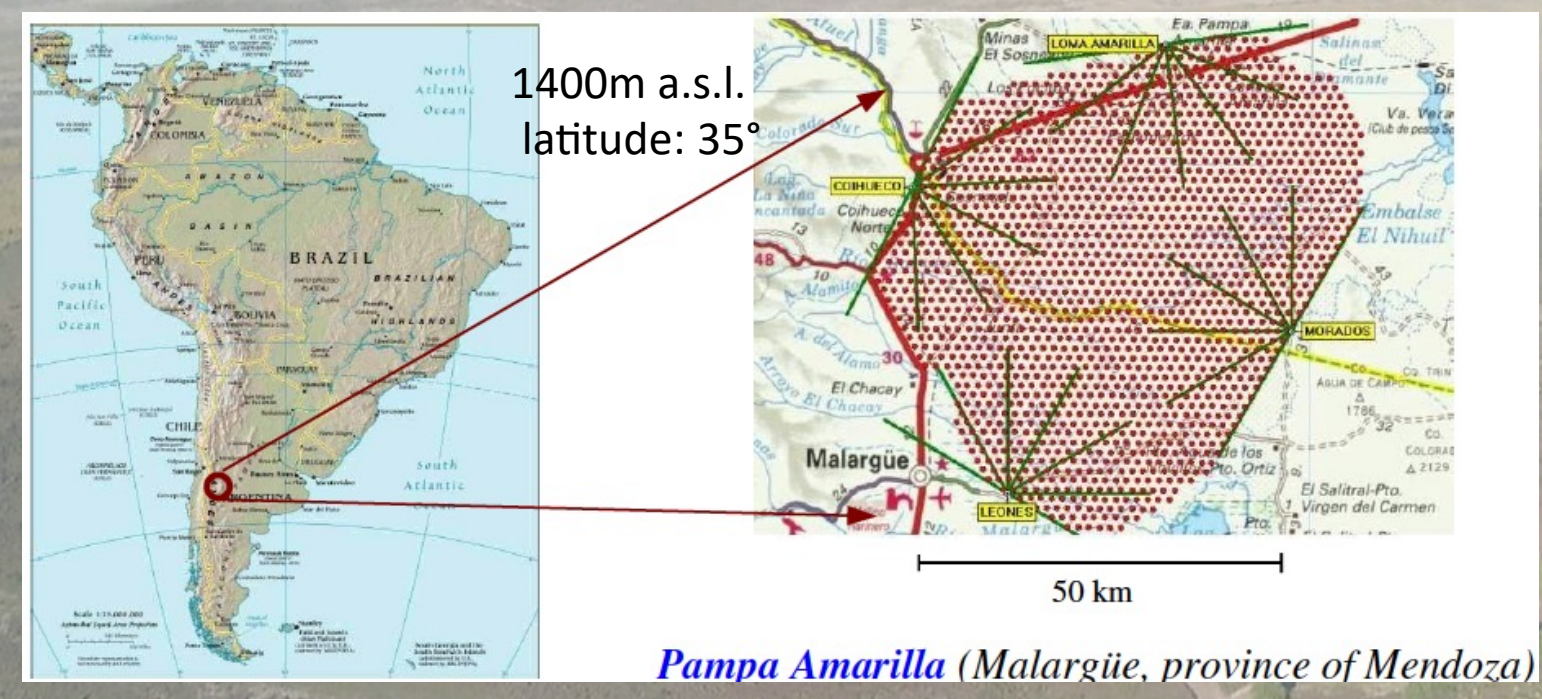


Figure 3. The left part shows the two HiRes monocular spectra in red and black. In addition the Fly's Eye stereo spectrum is shown in blue and the HiRes/MIA spectrum is green. The right part shows the two HiRes monocular spectra in red and black, plus the original AGASA spectrum in blue and the 2005 Auger spectrum in magenta.



The Pierre Auger Observatory



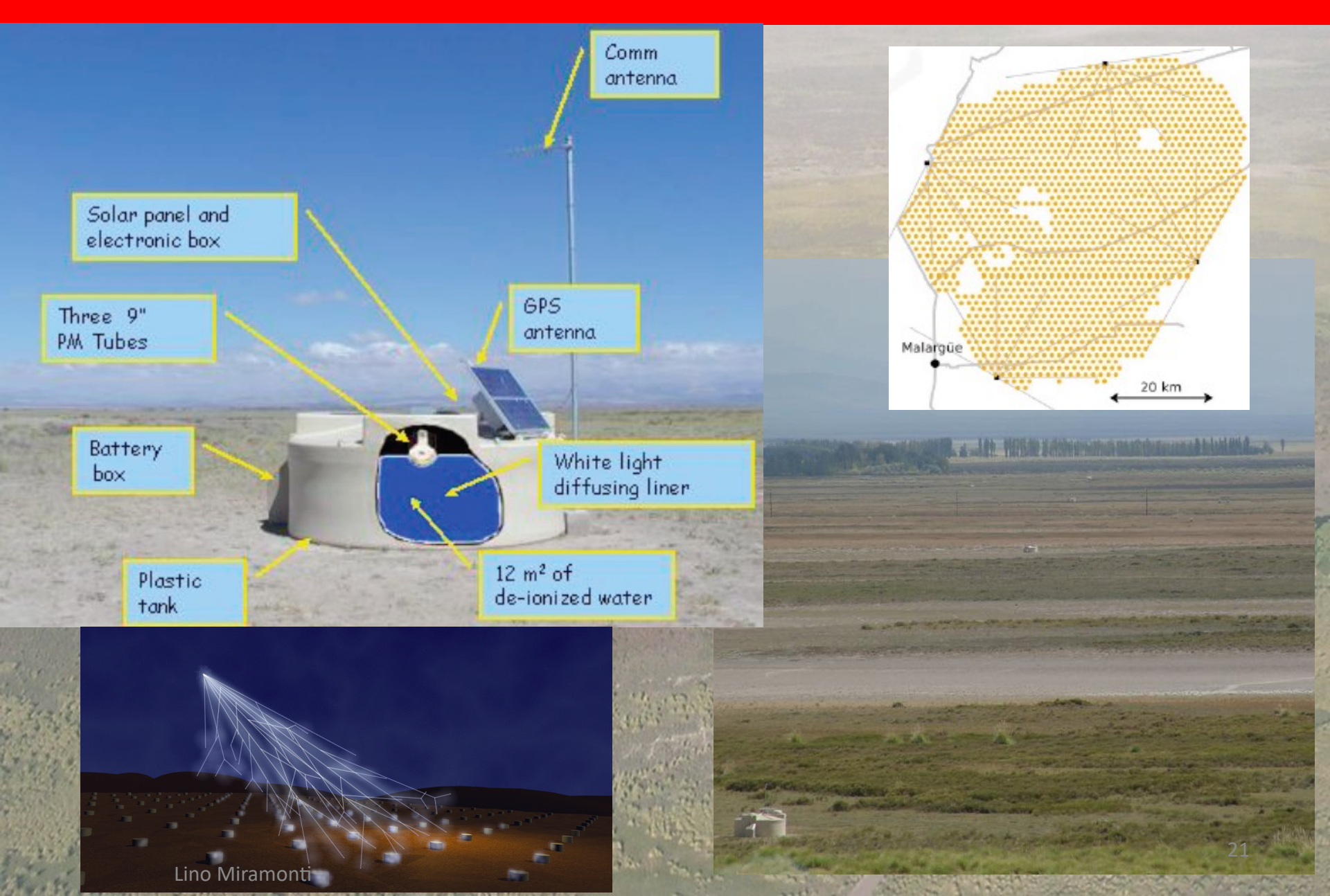


Physics data since 2004,

1600 water Cherenkov tanks (1.5 km distance in a triangular grid) = 3000 km²

24 fluorescence telescopes stations (4 building)

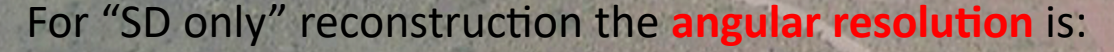
SURFACE DETECTOR ARRAY



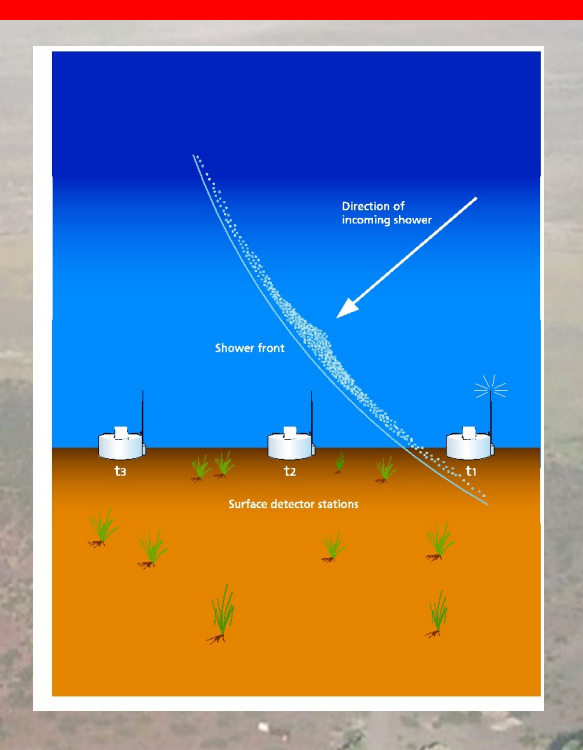
SURFACE DETECTOR ARRAY

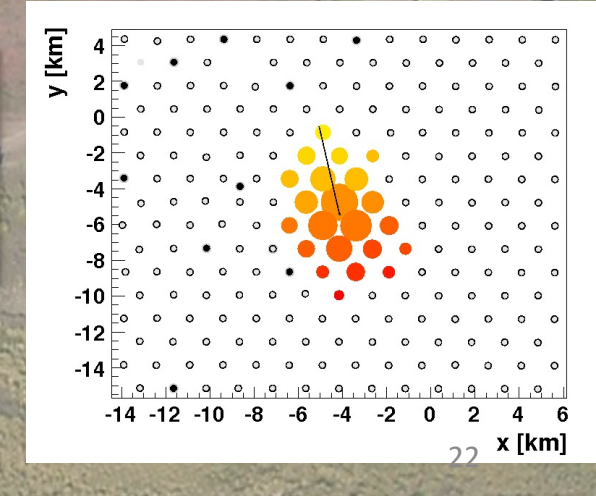
SD geometry reconstruction

The reconstruction of arrival direction of primary cosmic rays is obtained by fitting the arrival times sequence of particles in shower front.



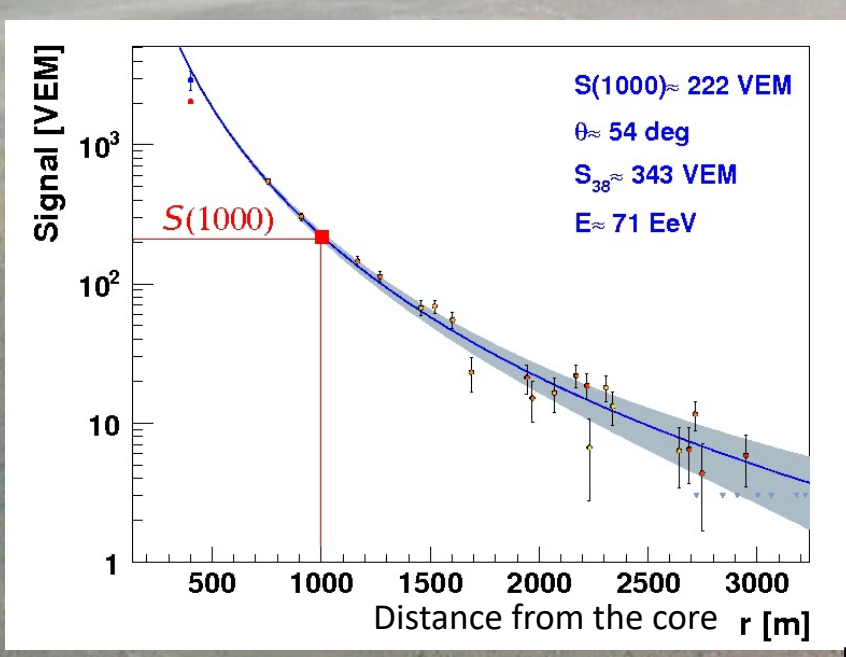
Better than 2.2°	3-fold events	E < 4 EeV
Better than 1.7°	4-fold events	3 < E < 10 EeV
Better than 1.4°	For higher multiplicity	E > 8 EeV





SURFACE DETECTOR ARRAY

SD energy determination



VEM: Vertical Equivalent Muon

The SD is full efficient from 3 1018 eV

Energy estimator: **S(1000)** that is the particle density at 1000 m from shower axis

Lateral Distribution Function (LDF)

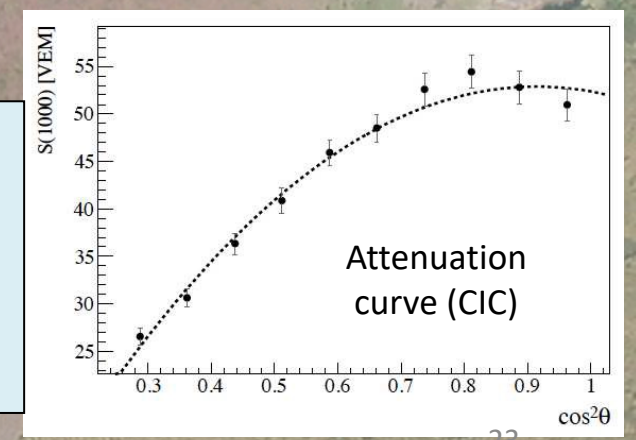
$$S(r) = S(1000) \left(\frac{r}{1000}\right)^{-\beta} \left(\frac{r + 700}{1700}\right)^{-\beta}$$

S(1000) is converted into \$38 that is the S(1000) that a shower would have produced if it had arrived with a zenith angle of 38°

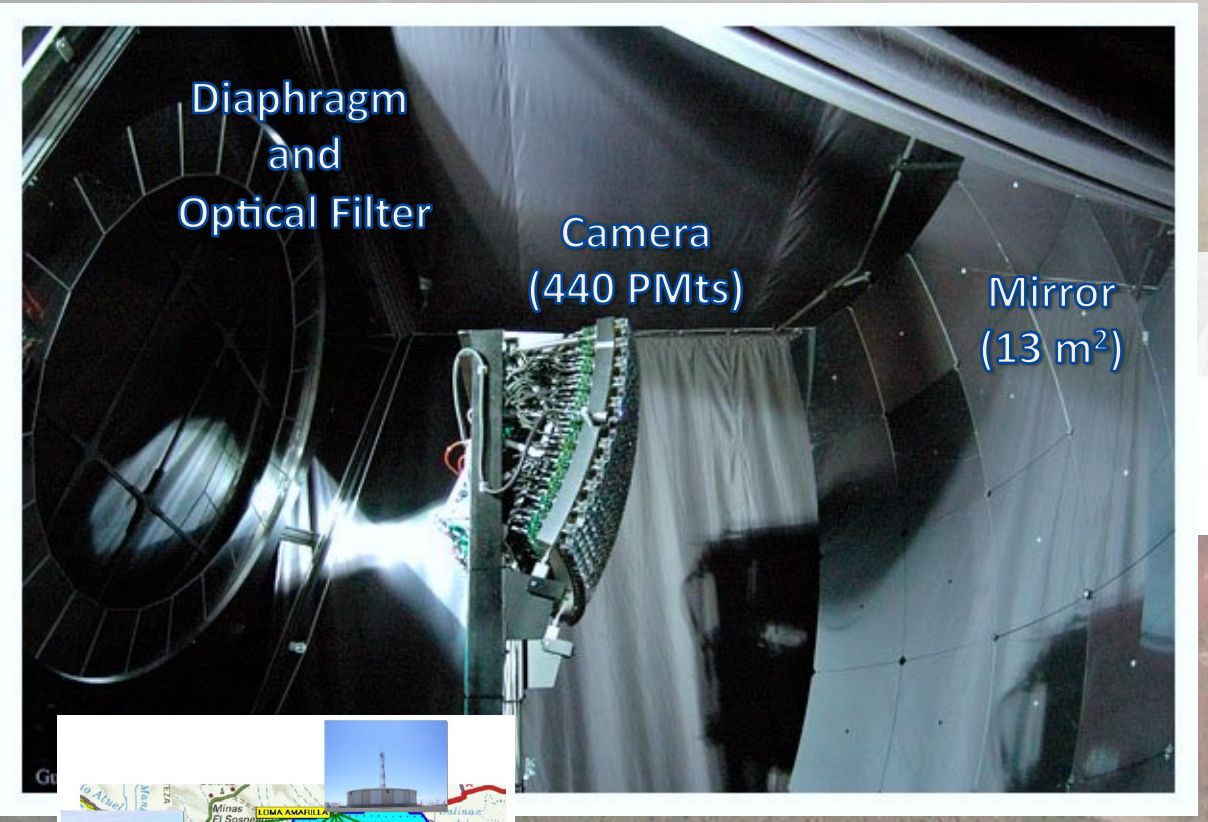
$$CIC(\theta) = 1 + ax + bx^{2}$$

$$x = \cos^{2}\theta - \cos^{2}38^{\circ}$$

$$S38 = \frac{S(1000)}{CIC(\theta)}$$



FLUORESCENCE DETECTOR



~ 60 km o Miramonti



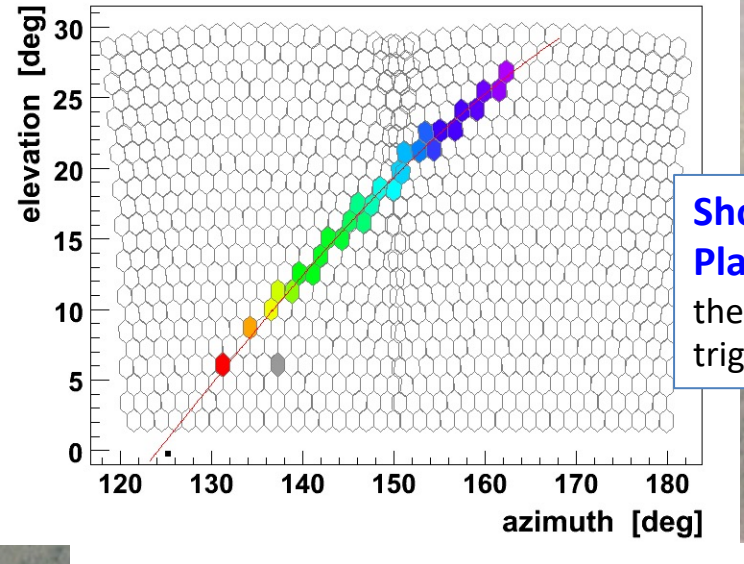
24 Fluorescence telescopes in 4 buildings:

Mirrors: 3.6 m x 3.6 m with field of view 30° x 30° from 1° to 31° in elevation.

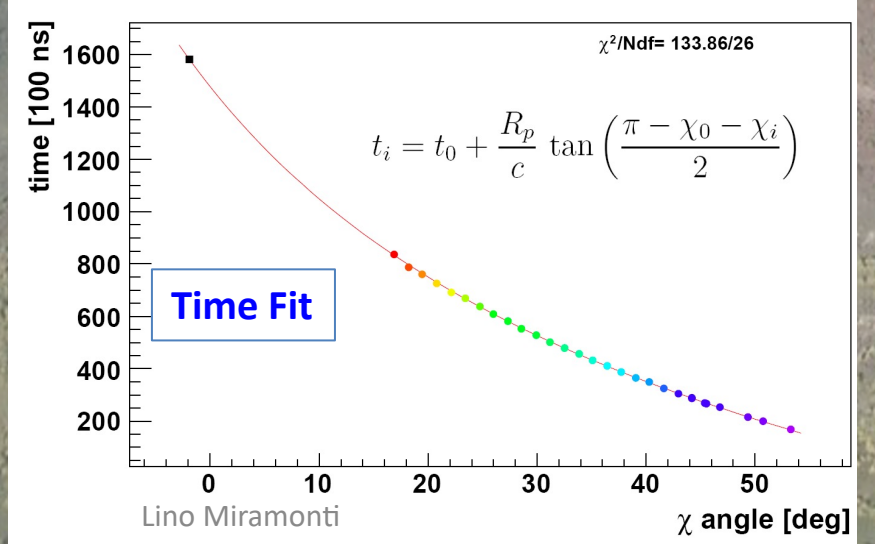
Each telescope is equipped with 440 photomultipliers.

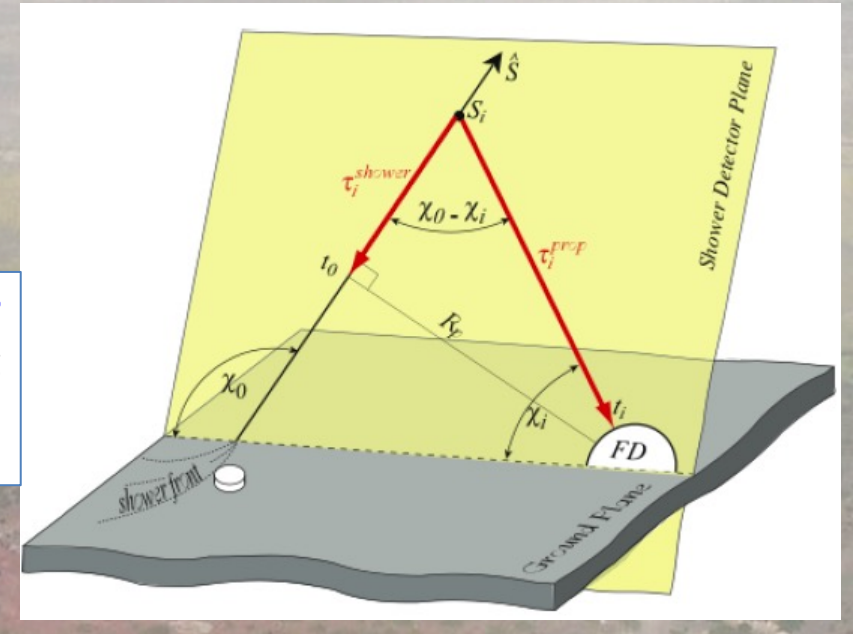
FLUORESCENCE DETECTOR

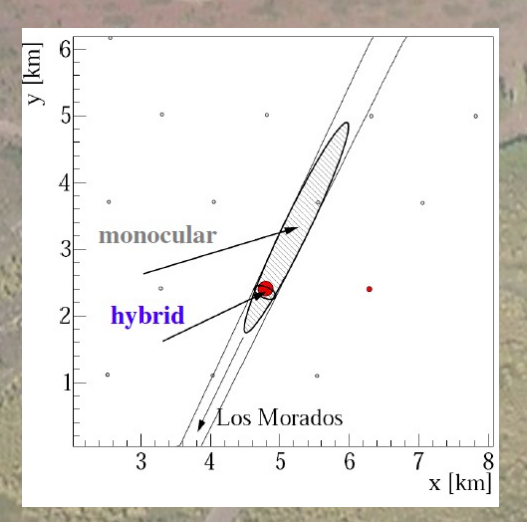
FD geometry reconstruction



Shower Detector Plane (SDP) using the directions of the triggered pixels



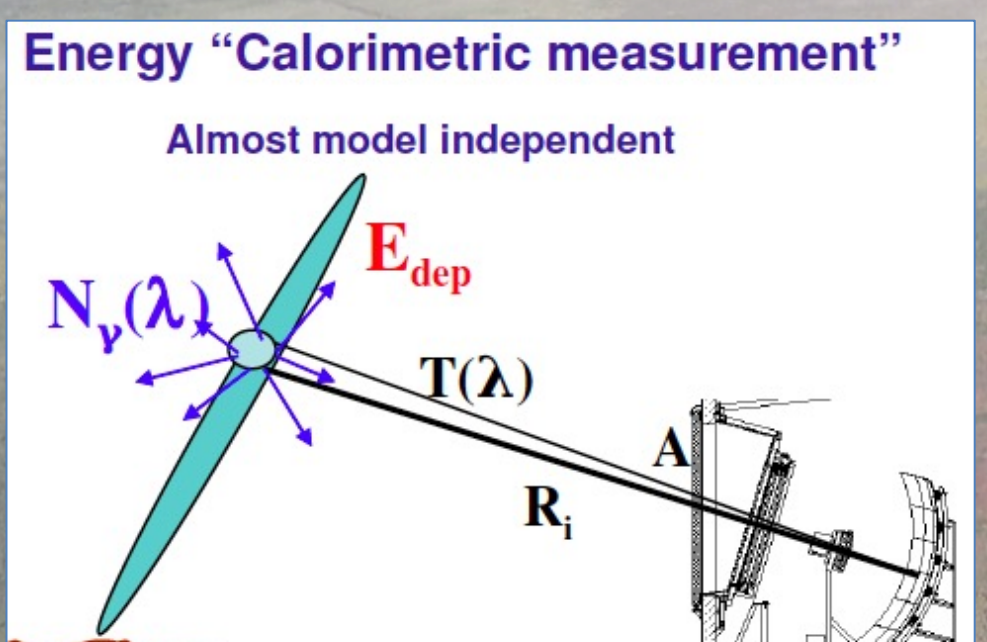


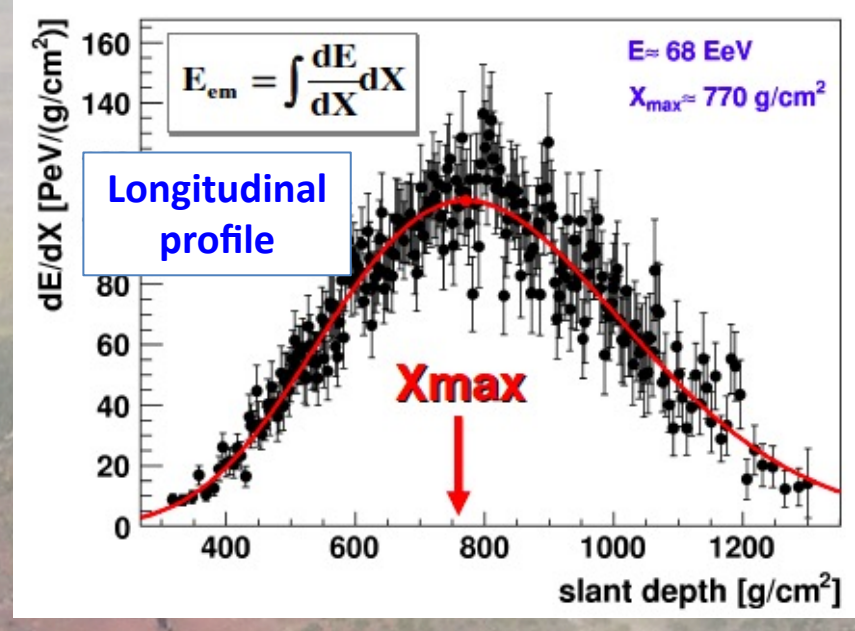


In the PAO the reconstruction of direction is performed in hybrid mode (see later)

FLUORESCENCE DETECTOR

FD energy determination





The number of photons $N_{\gamma}(\lambda)$ is proportional to the deposited Energy E_{dep} (from laboratory measurements – Fluorescence yield)

- Geometry n° of photons in the FD FOV depend on A/R_i²
- Atmosphere n° of photons at diaphragm depend on $T(\lambda)$
- The ADC count depend on Detector Calibration

Facilities in the field to monitor the transparency of the air and the cloud coverage



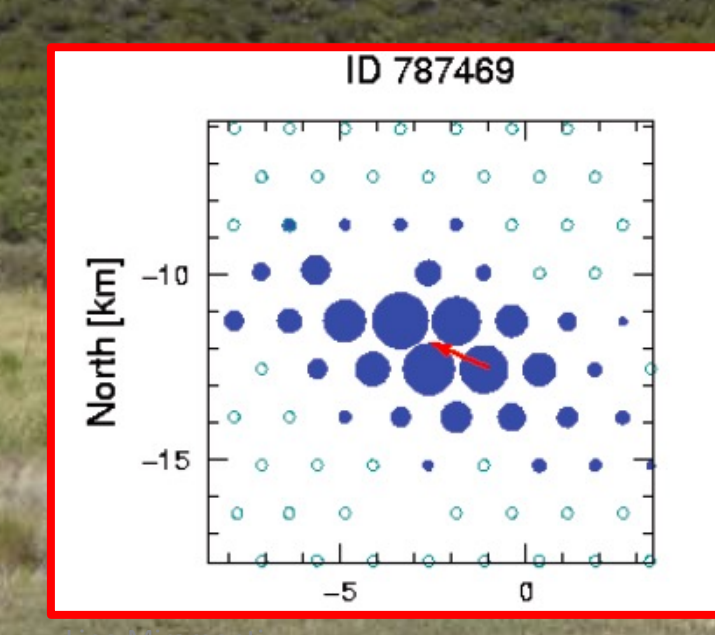
The Hybrid Concept

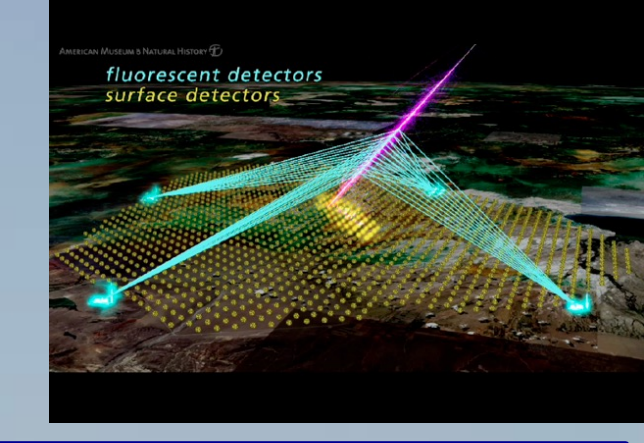
SD and FD combined in the hybrid mode

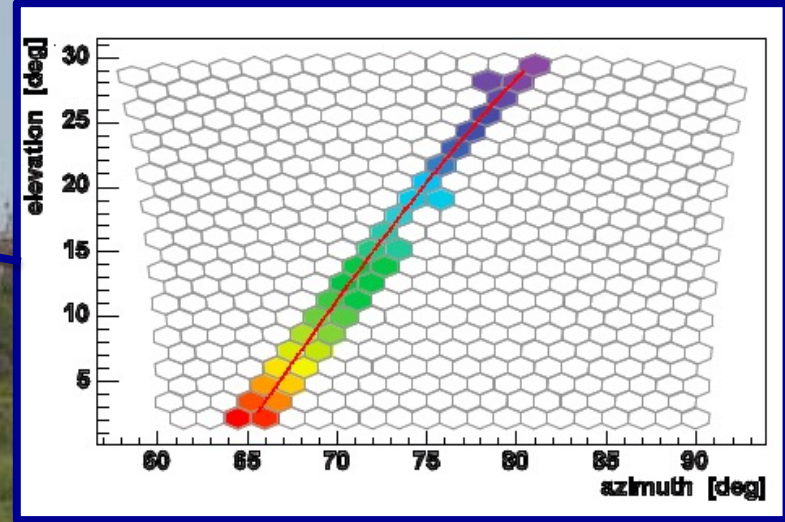
(i.e. FD + at least 1 SD station)

Accurate <u>energy and direction</u> measurement and

Mass composition studies in a complementary way





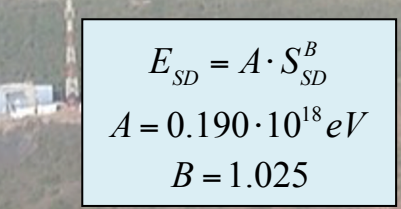


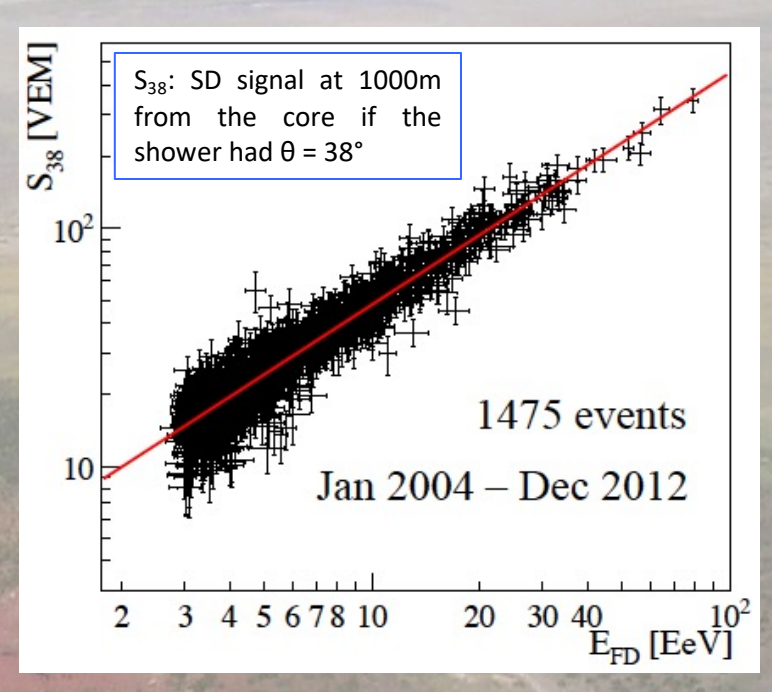
The Hybrid Concept

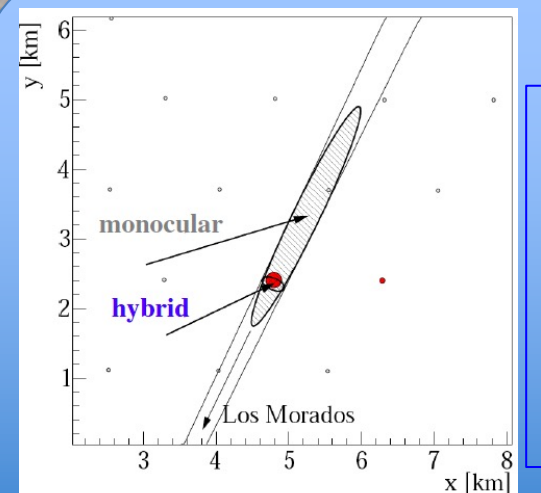
Energy Calibration for SD events using golden hybrid data (FD $+ \ge 3$ SD stations)

Using hybrid events, the SD energy estimator S38 is calibrated without relying on Monte Carlo simulation with an accuracy of 14%

AND AND ADDRESS OF THE PERSON		
Absolute fluorescence yield	3.4%	
Fluores. spectrum and quenching param.	1.1%	
Sub total (Fluorescence Yield)	3.6%	
Aerosol optical depth	3% ÷ 6%	
Aerosol phase function	1%	
Wavelength dependence of aerosol scattering	0.5%	
Atmospheric density profile	1%	
Sub total (Atmosphere)	3.4% ÷ 6.2%	
Absolute FD calibration	9%	
Nightly relative calibration	2%	
Optical efficiency	3.5%	
Sub total (FD calibration)	9.9%	
Folding with point spread function	5%	
Multiple scattering model	1%	
Simulation bias	2%	
Constraints in the Gaisser-Hillas fit	3.5% ÷ 1%	
Sub total (FD profile reconstruction)	6.5% ÷ 5.6%	
Invisible energy	3% ÷ 1.5%	
Statistical error of the SD calib. fit	0.7% ÷ 1.8%	
Stability of the energy scale	5%	
TOTAL	14%	







Geometry Reconstruction

Thanks to hybrid mode:

The Hybrid angular resolution is ≈ 0.6°

and

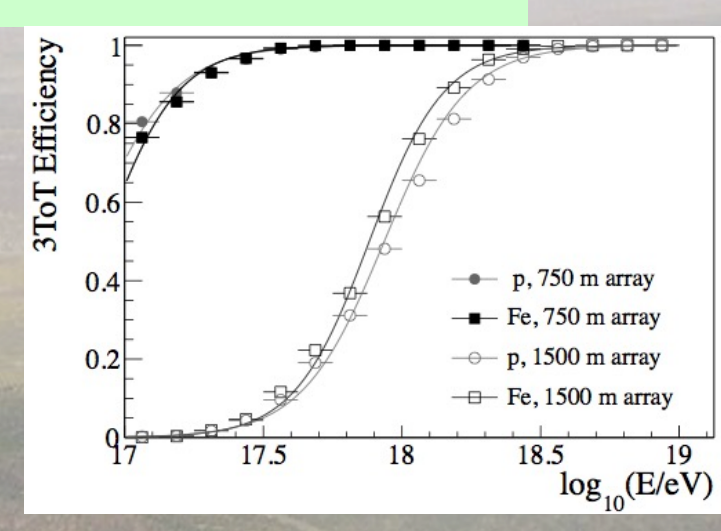
The core resolution is ≈ 50 meters

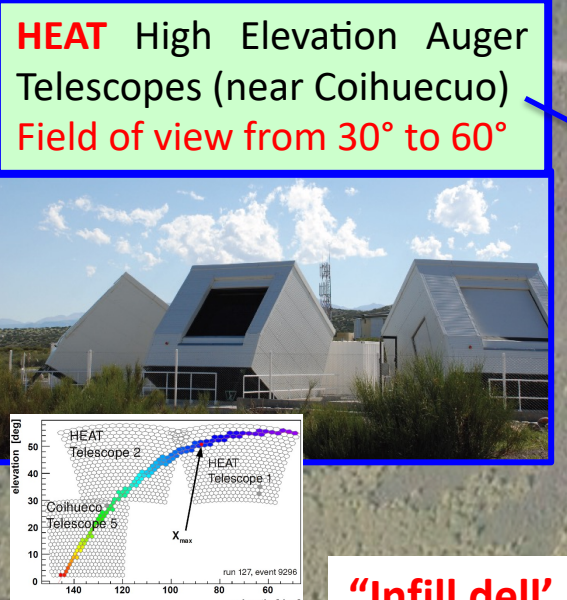
The Pierre Auger Enhancements

The SD array is fully efficient at energies above 3 1018 eV

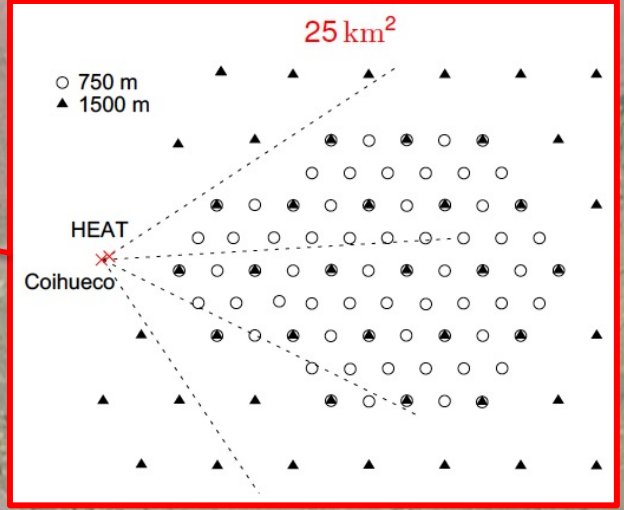
The transition from galactic to extra-galactic cosmic rays may occur between 10^{17} eV and the ankle (4 10^{18} eV). A precise measurement of the flux at energies above 10^{17} eV is important for discriminating between different theoretical models

49 additional detectors with 750 m spacing have been nested within the 1500 m array to cover an area of about 25 km²: **INFILL** has a full efficiency above 3 10¹⁷ eV







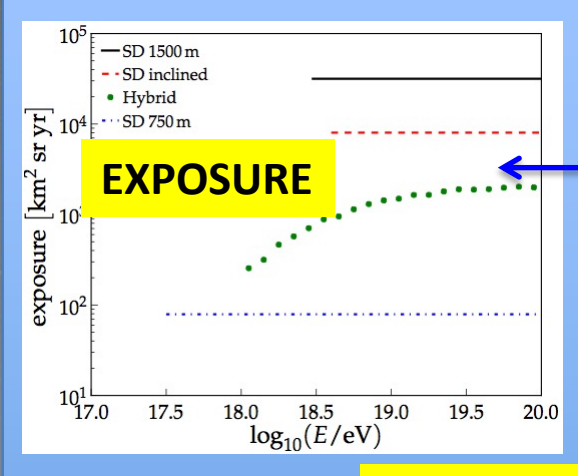


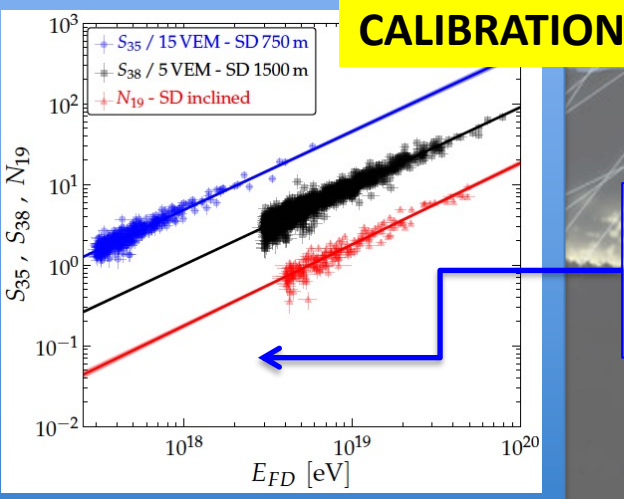
"Infill dell' Infill" 433 m full efficiency above 3 10¹⁶ eV (deployment > 2019)

Results of the Pierre Auger Observatory

The measurement of the energy spectrum of cosmic rays above 3 10¹⁷ eV Combining the SD regular array data and the INFILL array data (plus)

The **exposure** and the **calibration** are different for the different data sets





Lino Miramonti

Correlation between the different energy estimators S_{38} , S_{35} and N_{19} and the energy determined by FD.

Combining the SD regular array data and the INFILL array data (plus the hybrid ones) it is possible to obtain the measurement of the cosmic ray flux starting from 3 10¹⁷ eV.

The dataset extends from 1 January 2004 to 31 December 2012.

Integrated exposure of the different detectors at the Pierre Auger Observatory as a function of energy. We have to distinguish between **vertical events** ($\vartheta < 60^{\circ}$) and **inclined events** ($62^{\circ} \le \vartheta < 80^{\circ}$)

	Auger SD			Auger hybrid
	1500 m vertical	1500 m inclined	750 m vertical	
Data taking period	01/2004 - 12/2012	01/2004 - 12/2012	08/2008 - 12/2012	11/2005 - 12/2012
Exposure [km ² sr yr]	31645 ± 950	8027 ± 240	79 ± 4	see Fig. 1
Zenith angles [°]	0 - 60	62 - 80	0 - 55	0 - 60
Threshold energy E_{eff} [eV]	3×10^{18}	4×10^{18}	3×10^{17}	10^{18}
No. of events $(E > E_{\text{eff}})$	82318	11074	29585	11155
No. of events (golden hybrids)	1475	175	414	-
Energy calibration (A) [EeV]	0.190 ± 0.005	5.61 ± 0.1	$(1.21 \pm 0.07) \cdot 10^{-2}$	-
Energy calibration (B)	1.025 ± 0.007	0.985 ± 0.02	1.03 ± 0.02	-

Energy estimators: S₃₈ and S₃₅

The equivalent signal at median zenith angle of 38° (35°) is used to infer the energy for the 1500 m (750 m) array

Energy estimator for inclined air-showers: N₁₉

Inclined air-showers are characterized by the dominance of secondary <u>muons at ground</u>, as the electromagnetic component is largely absorbed in the large atmospheric depth traversed by the shower.

The reconstruction is based on the estimation of the relative muon content N_{19} with respect to a simulated proton shower with energy $10^{19}\,\text{eV}$

The measurement of the energy spectrum of cosmic

rays above 3 10¹⁷ eV

To characterize the spectral features, data are described with a <u>power law</u> below the ankle

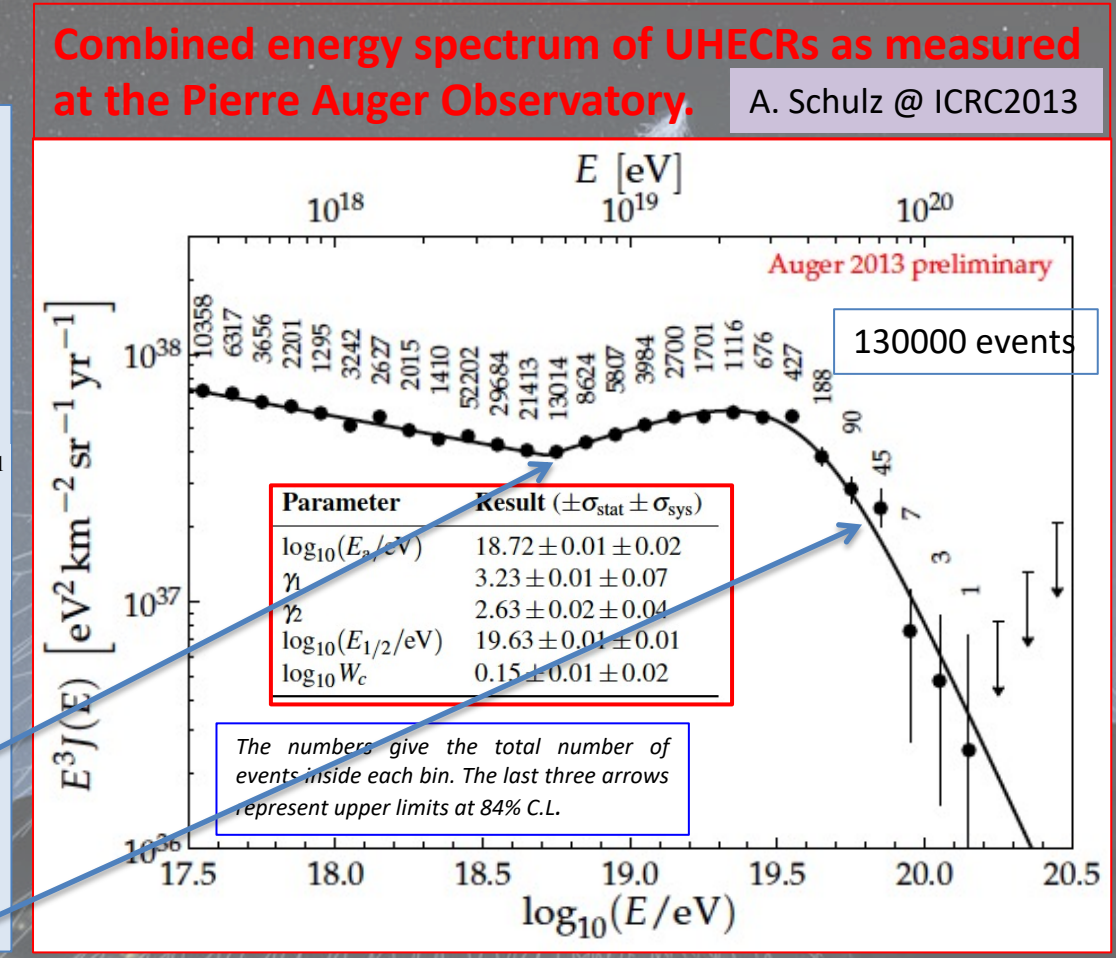
$$J(E) \propto E^{-\gamma_1}$$

and a <u>power law with smooth suppression</u> above

$$J(E; E > E_a) \propto E^{-\gamma_2} \left[1 + \exp\left(\frac{\log_{10} E - \log_{10} E_{\frac{1}{2}}}{\log_{10} W_c}\right) \right]^{-1}$$

 γ_1 , γ_2 are the spectral indices below/above the ankle at E_a .

 $E_{1/2}$ is the energy at which the flux has dropped to half of its peak value before the suppression, the steepness of which is described with $log_{10}W_c$.



- A. The ankle has been clearly seen
- B. The suppression in the flux of UHECRs has been firmly established with (>20 σ)

The measurements of the depth of shower maximum for the study of mass composition Mass determination is mandatory to

There are <u>several ways to study the</u> <u>composition</u> of the primary cosmic rays:

- a) X_{max} measurement
- b) muon production depth
- c) rise-time asymmetry measurements

The best way (smallest systematic uncertainties) is to measure the X_{max} distribution using fluorescence telescopes in hybrid mode.

Good data

taking conditions

Almost unbiased

Xmax distributions

Good Xmax

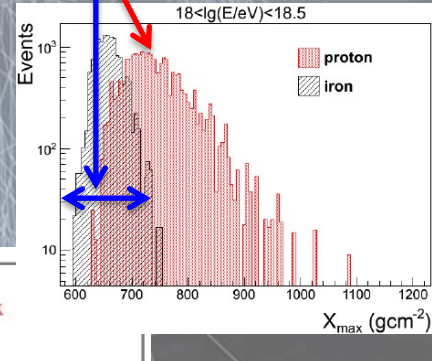
and Energy

measurement

Superposition principle:

Iron shower of energy E "is equal to" 56 proton showers of E/56

- proton showers penetrate deeper → higher X_{max}
- iron showers have less fluctuations \rightarrow smaller RMS(X_{max})



reach reliable conclusion on energy

spectrum, sources and acceleration

Data selection and Quality Cuts

atmosphere and calibration

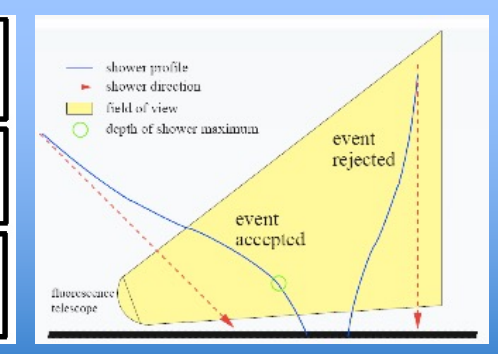
- good camera calibration constants
- require measured aerosol profile
- reject dust periods (VAOD@3km<0.1)
- cloud fraction < 25%

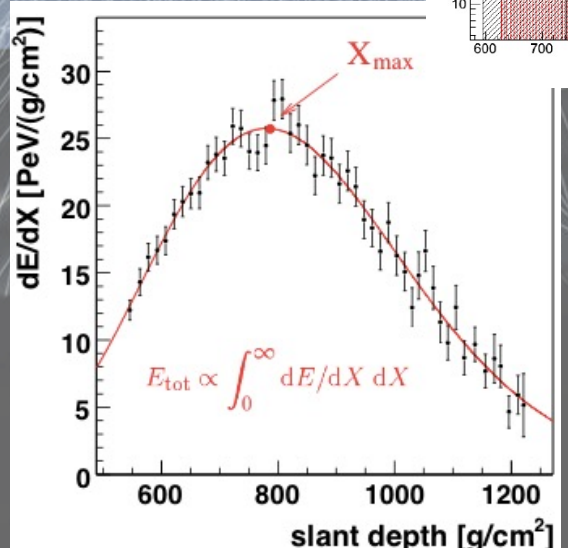
fiducial volume cuts

- · surface detector trigger probability
- · field of view
- minimum viewing angle > 20°

quality selection

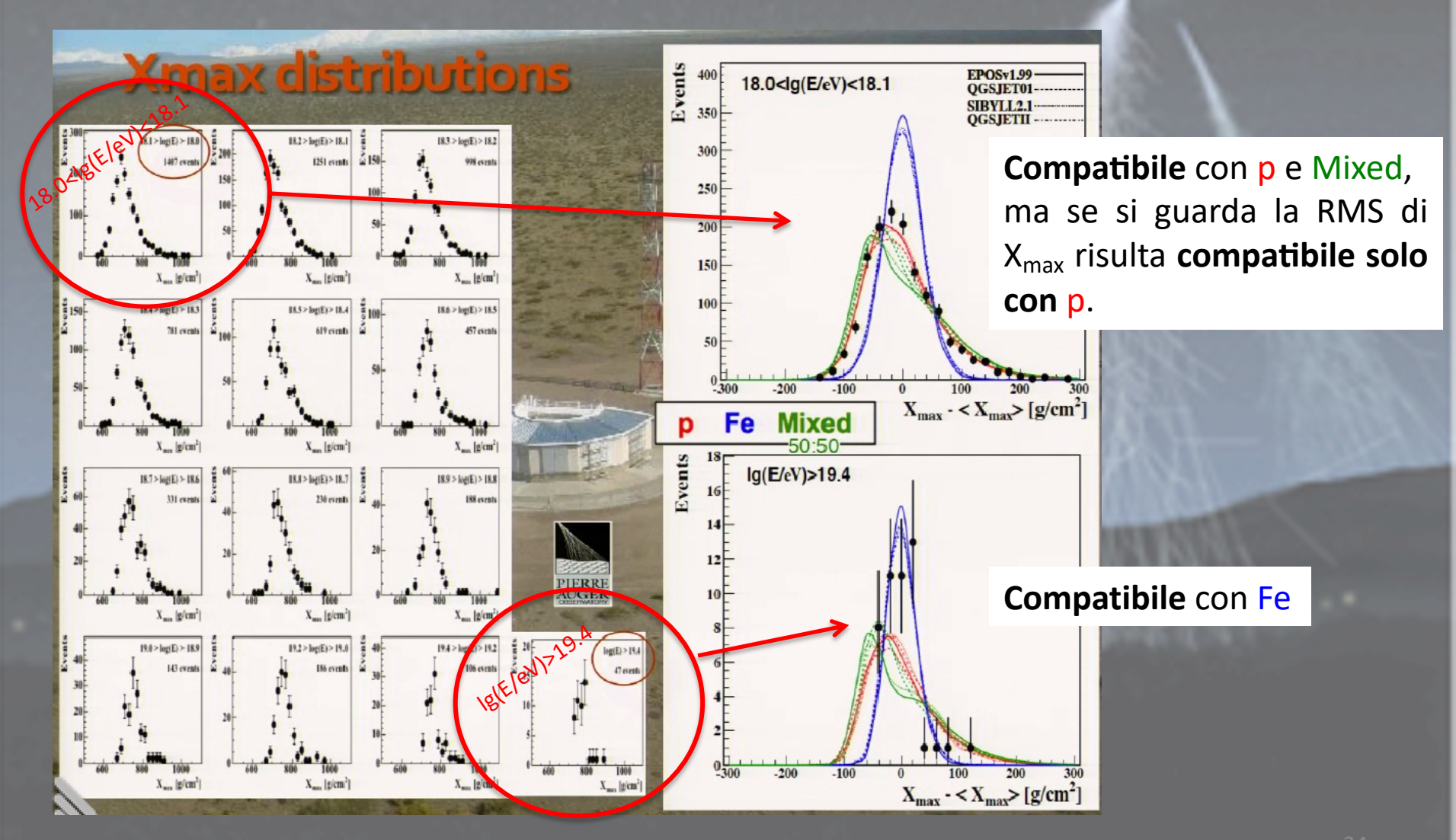
- · hybrid geometry reconstruction
- Xmax observed
- expected σ(Xmax) < 40 g/cm²
- reduced χ² of profile fit < 2.5





33

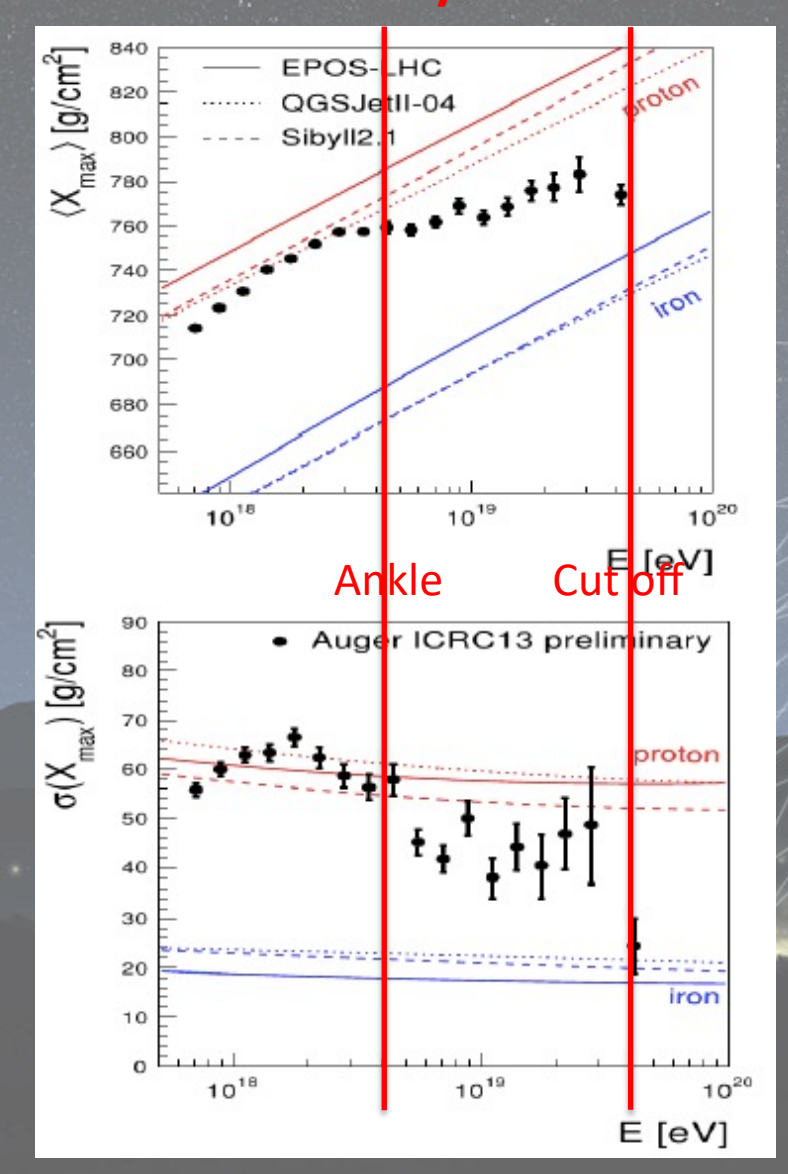
The measurements of the depth of shower maximum for the study of mass composition

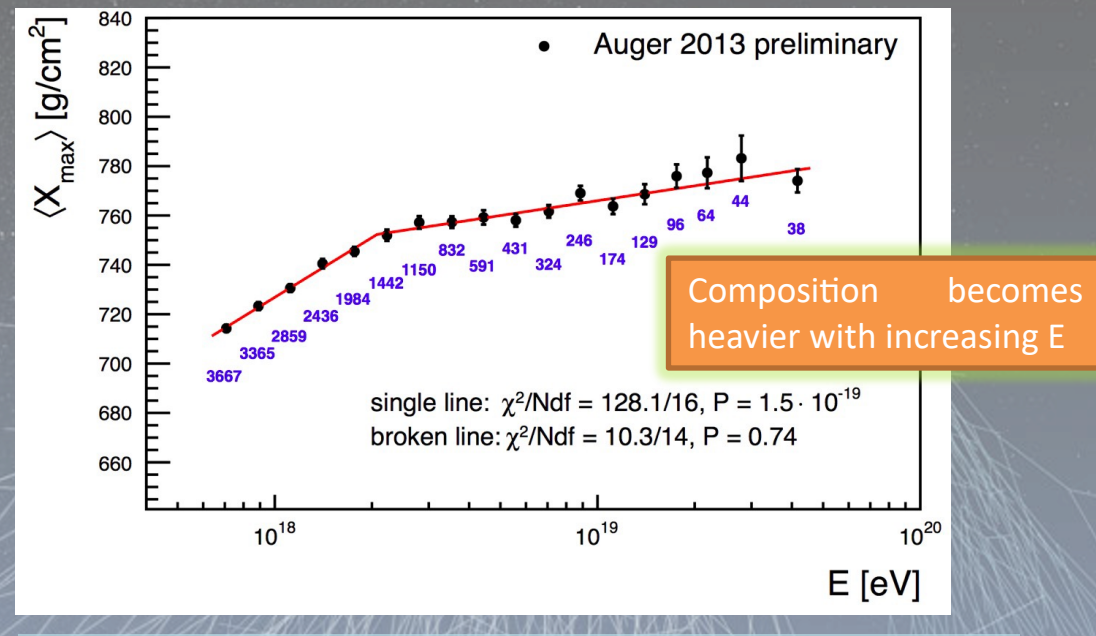


The measurements of the depth of shower maximum

for the study of mass composition

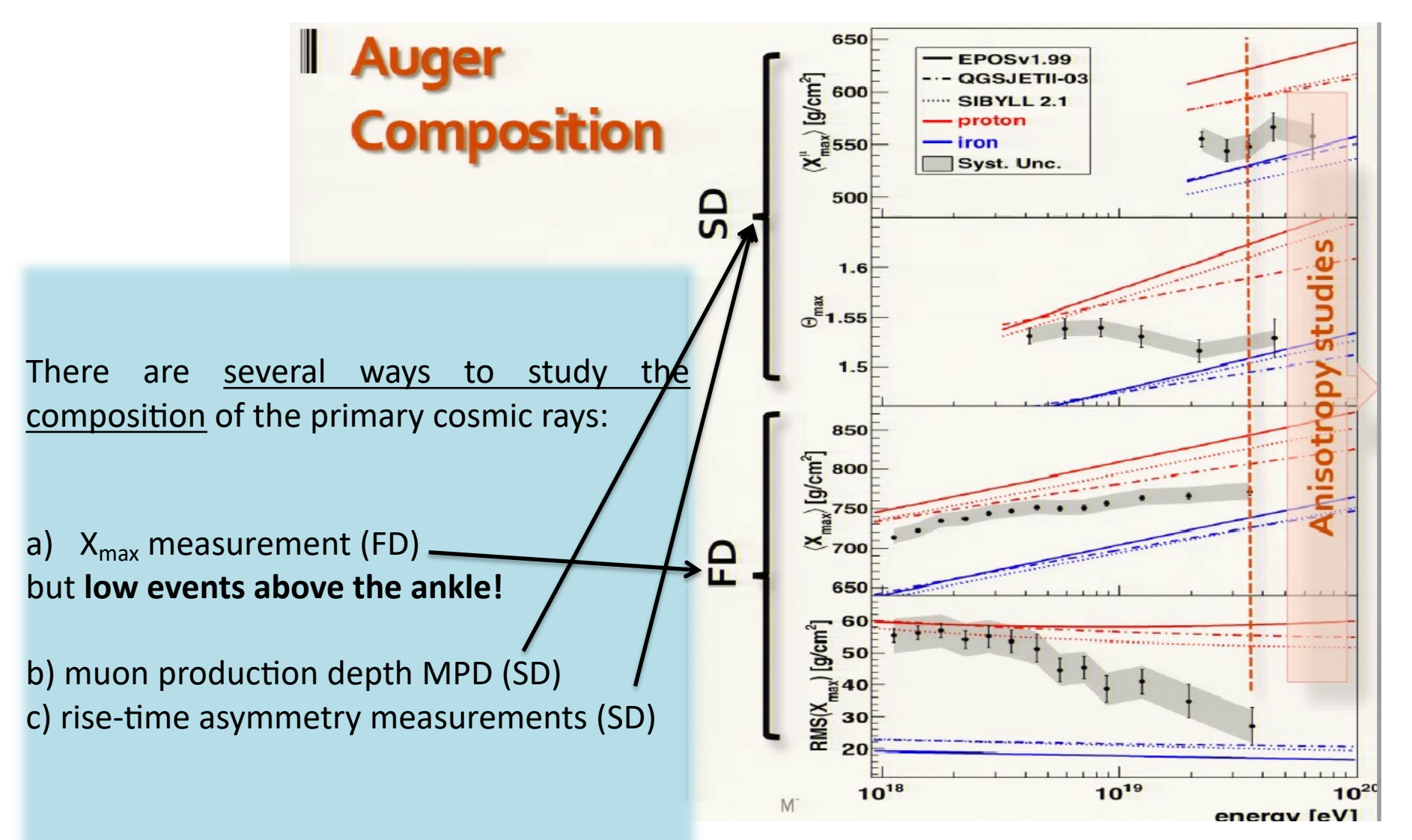
Vitor de Souza @ ICRC2013





- ✓ At low energy data is compatible with a significant fraction of protons
- ✓ <u>Break</u> on the elongation rate slope seems to <u>indicate a change in composition</u> towards a predominance of heavier nuclei at higher energies
- ✓ < X_{max} > and RMS(X_{max}) show similar trends towards heavy-like showers at high energies

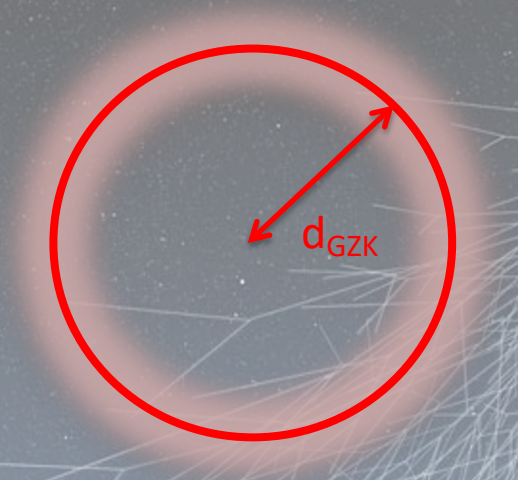
The measurements of the depth of shower maximum for the study of mass composition

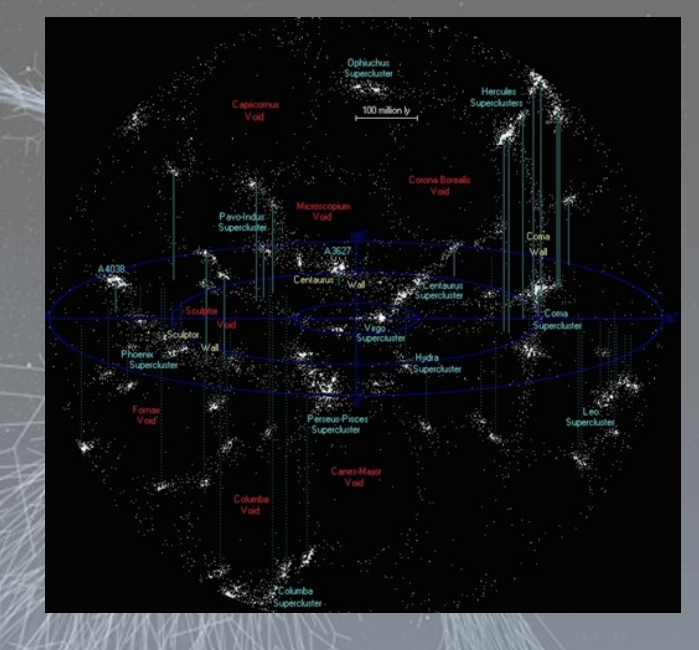


40

Anisotropy studies

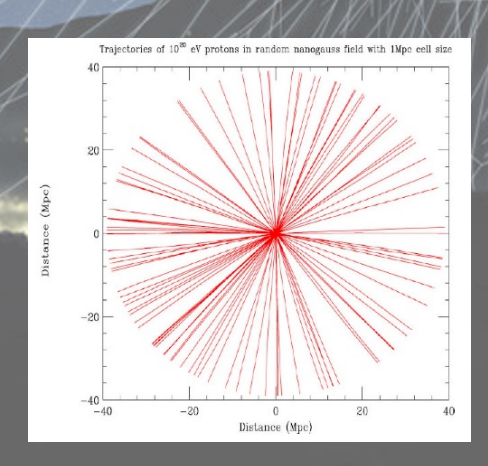
the observed cosmic ray flux suppression is interpreted in term of GZK-effect than the closest sources of UHECRs are situated within the GZK Volume of d_{GZK} < 100 Mpc (Within the GZK VOLUME the matter distribution in the Universe is inhomogeneous, and so must be the distribution of the UHECR sources)





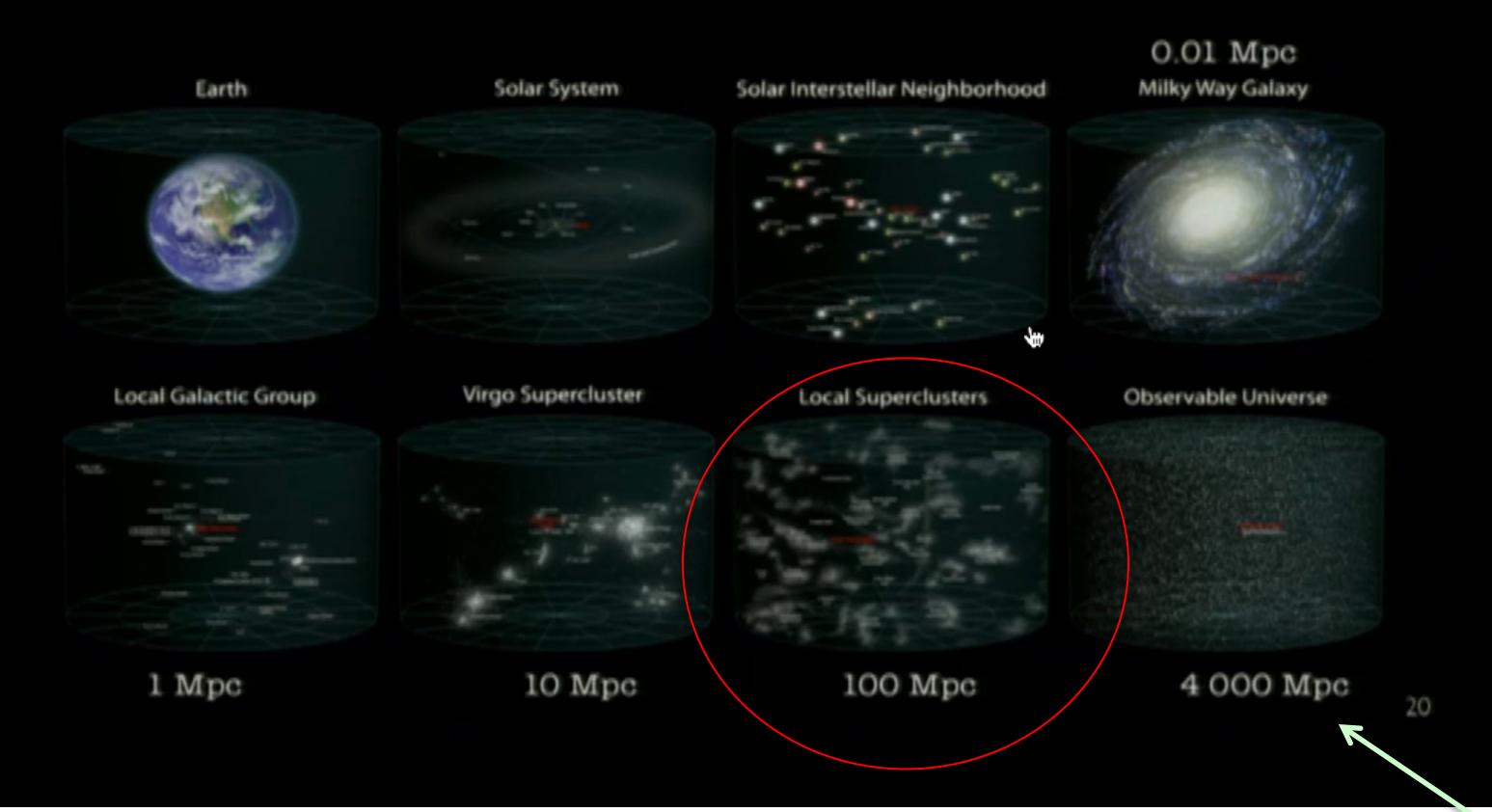
Then anisotropies would be expected.

If <u>propagation</u> of UHECRs at these distances is <u>quasi-rectilinear</u>



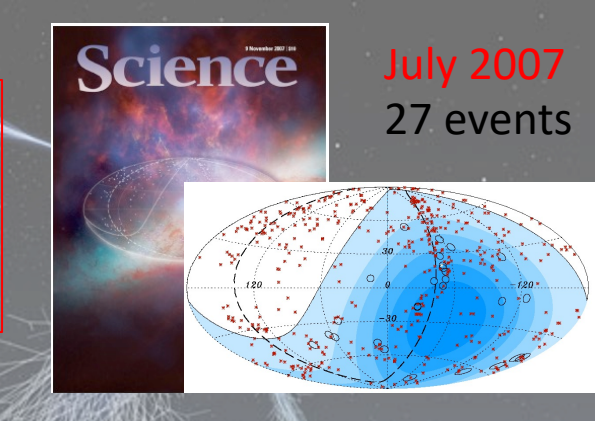
Quelles distances dans l'Univers ?

les rayons cosmiques de plus haute énergie proviennent de sources situées approx. à 4 - 100 Mpc



Universo Osservabile $13.7 Gy \rightarrow \frac{13.7 \cdot 10^9 anni}{3.26} = 4.2 \cdot 10^9 pc \approx 4000 Mpc$

In 2007; the Pierre Auger Collaboration reported directional correlations of UHECRs at E>55 EeV with AGN from the Véron-Cetty-Véron catalog within 75 Mpc on an angular scale of 3.1° at 99% CL.



From the 27 events collected up to July 2007 with energy greater than 55 EeV

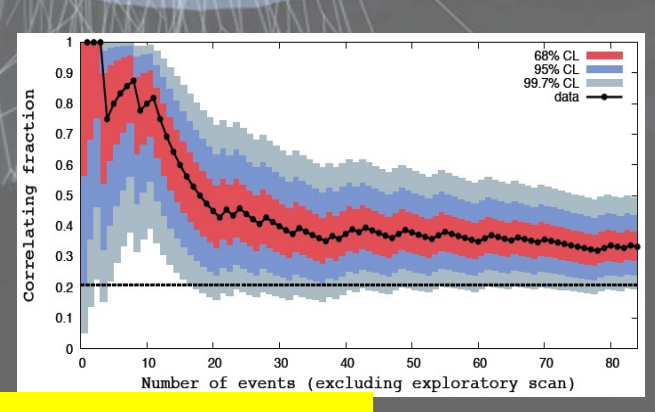
- (Period I) the firsts 14 events were used as exploratory scan in order to determine the optimal parameters.
- (*Period II*) among the remaining 13 events 9 events correlating with AGNs (to be compared with 2.7 events if they had been isotropic) corresponding to a correlation of (69⁺¹³₋₁₁)%.

Being the chance correlation p_{iso} = 21% the chance probability of observing such a correlation is 1.7 10⁻³.

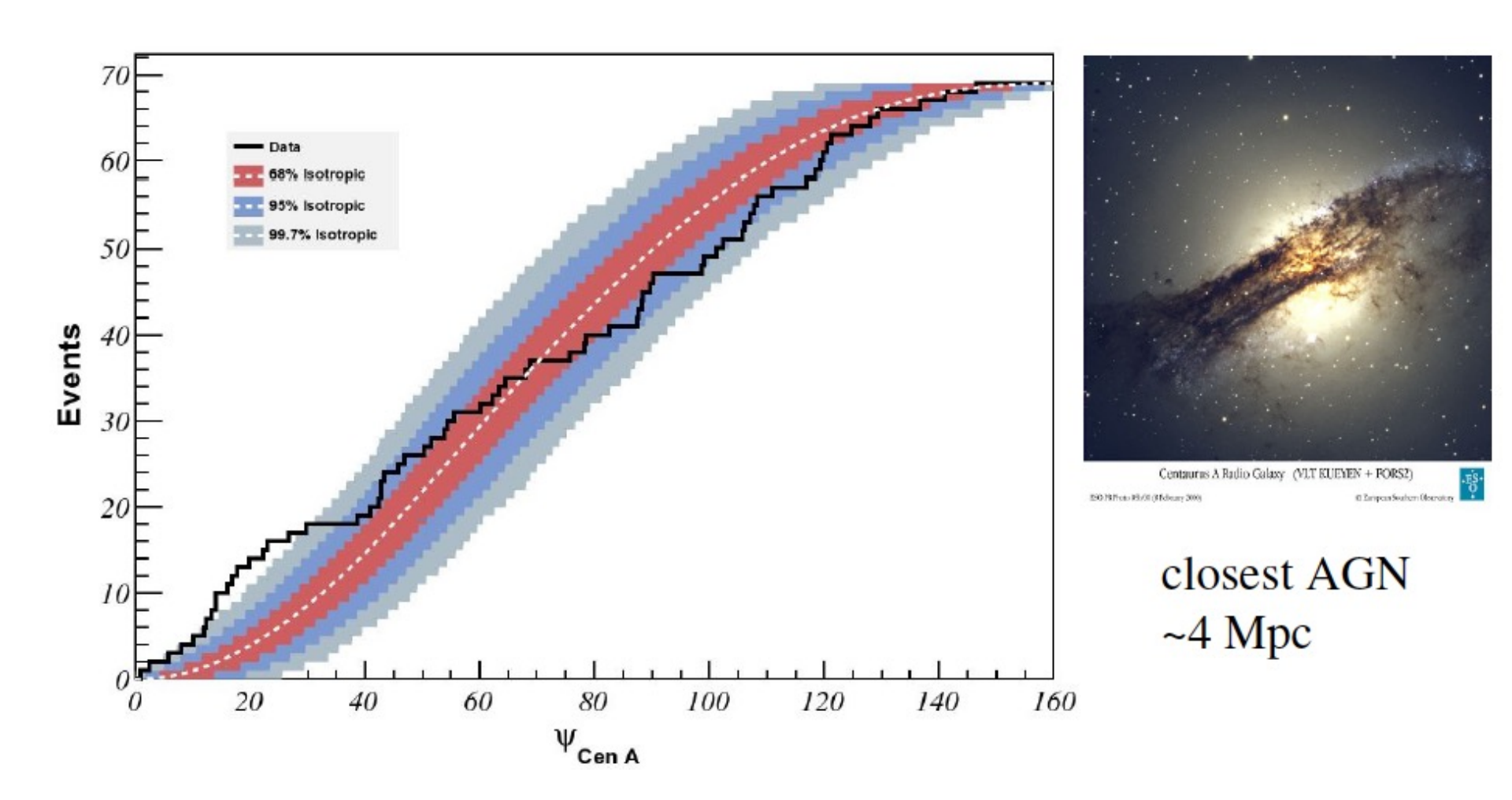
The latest update including data up to June 2011 which yields a total of 28 AGNs (to be compared with 17.6 events if they had been isotropic) of 84 events (Period II+III+IV) shows a correlation of (13.44).

The chance probability of observing such a correlation remain below 1%.

					11 1 1 11/8	A
			/////			ce interval does not contain the
	14 events	Period I (expl. scan)			hypothesised popul	ation value, then performing the
27 events					significance test	will lead to a p-value $\frac{<100-\Omega}{100}$
	13 events	Period II	9 correlating	(2.7 if iso)	$p_{data} = \frac{9}{13} = 0.69$	chance prob. $P = 1.7 \cdot 10^{-3}$
	84 events	Period II + III + IV	28 correlating		$p_{data} = \frac{28}{84} = 0.33$	<i>chance prob. P</i> = 0.006



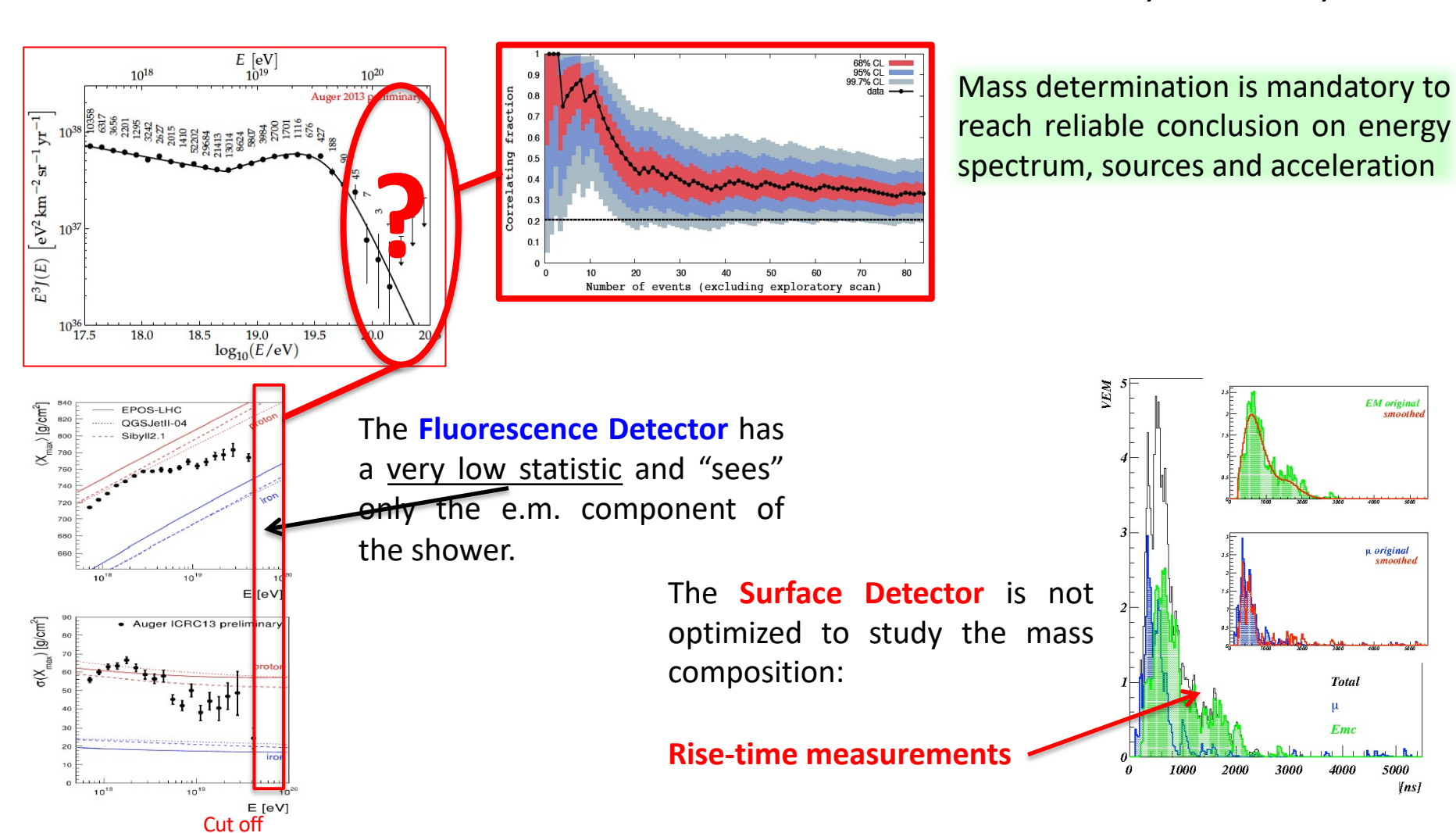
Directional correlation with Centaurus A?



cumulative distribution around Cen A:

at 18°: 13 observed, 3.2 expected from isotropy

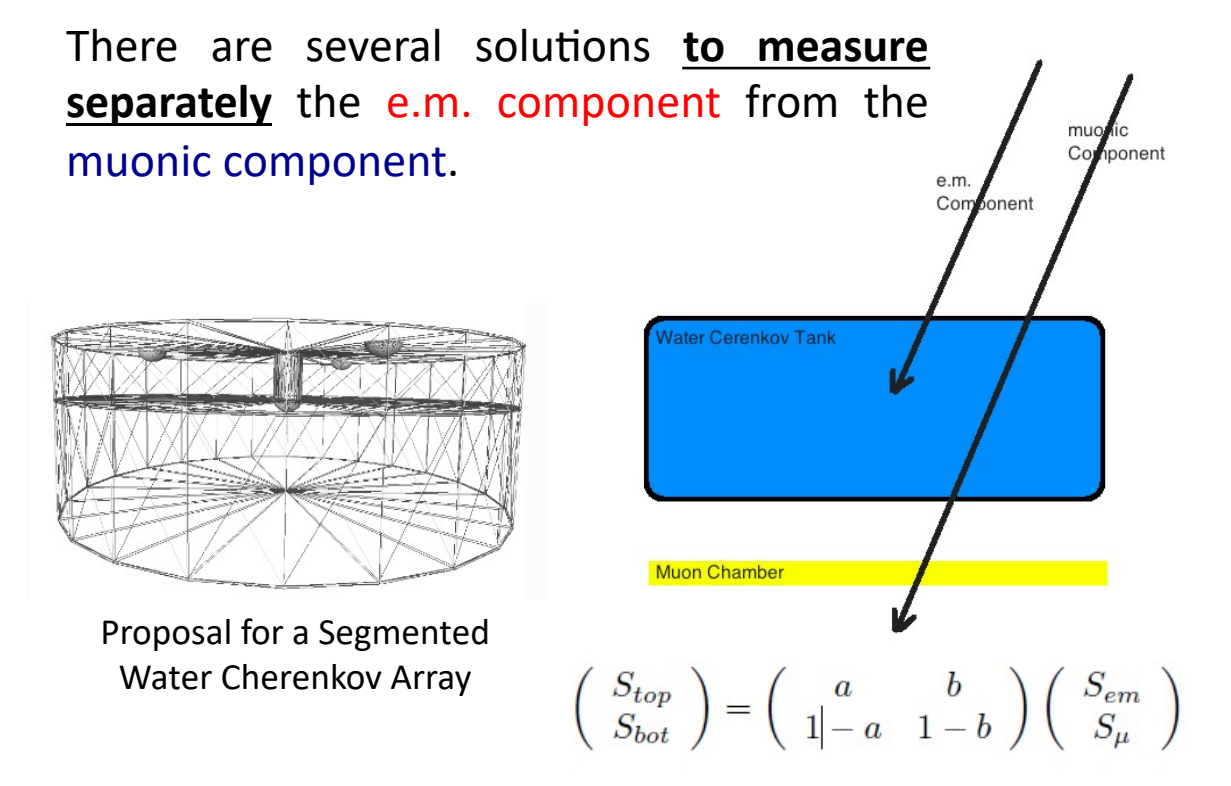
Proton Cosmic Ray Astronomy



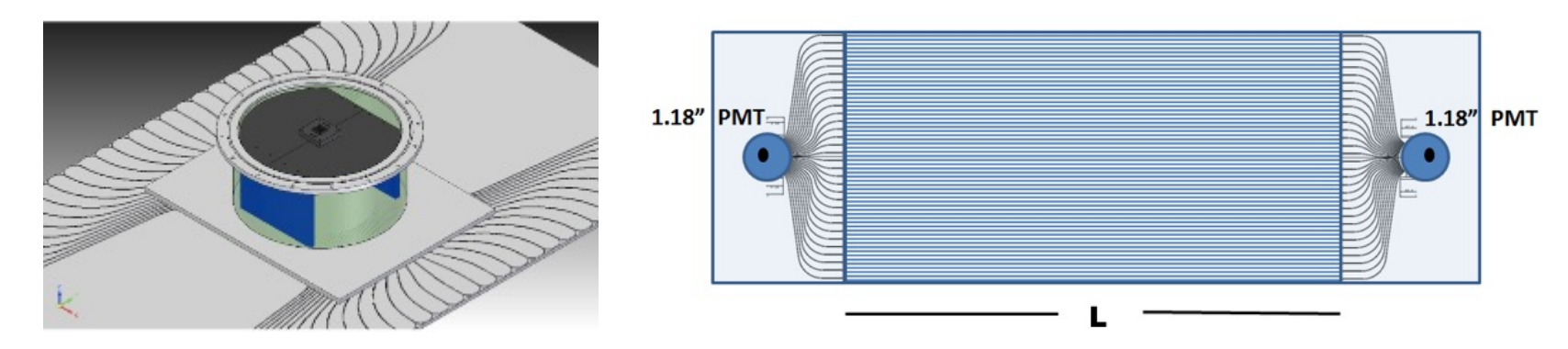
The e.m. component and the muonic component have to be measured separately!

Muon-E.M. Detectors

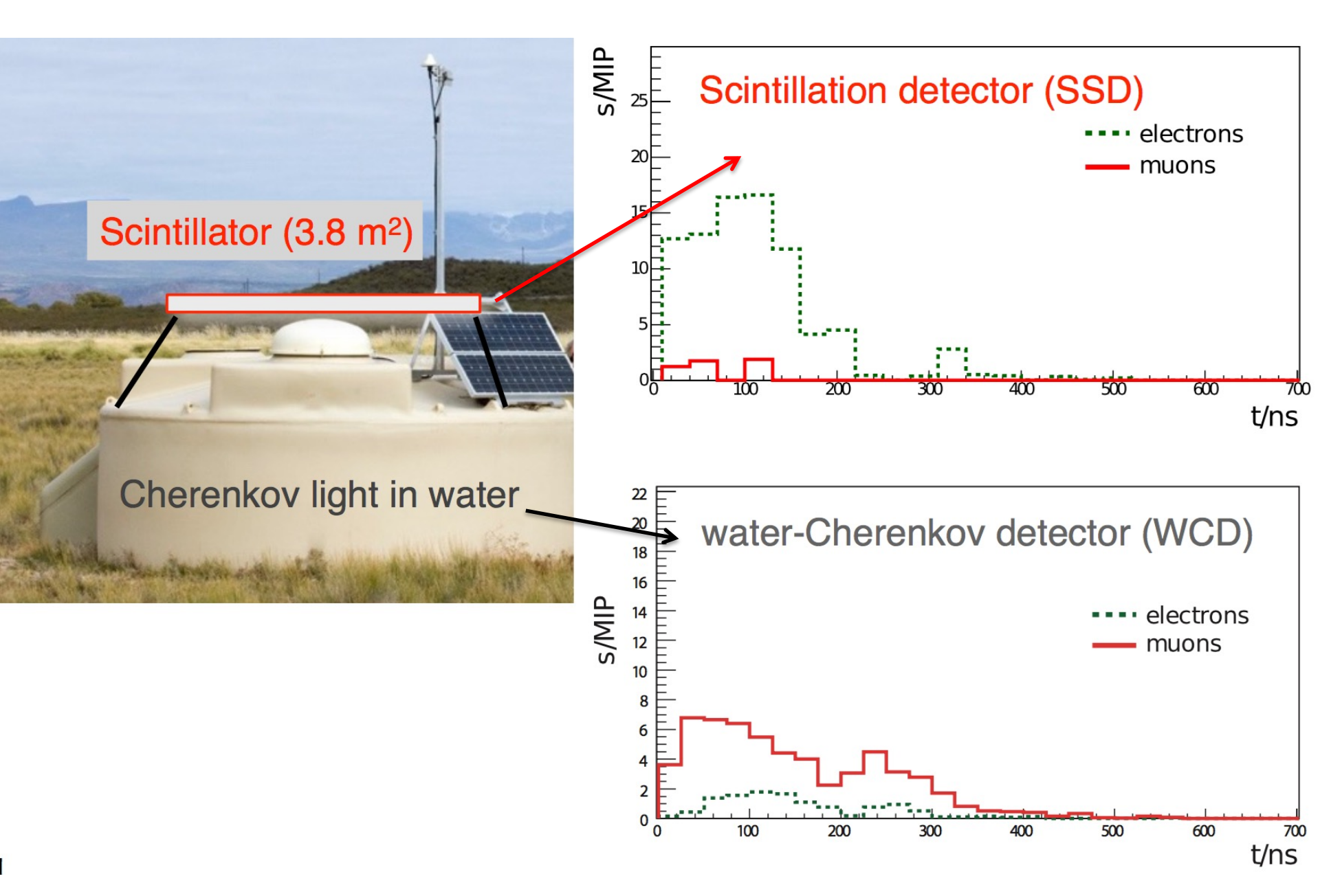




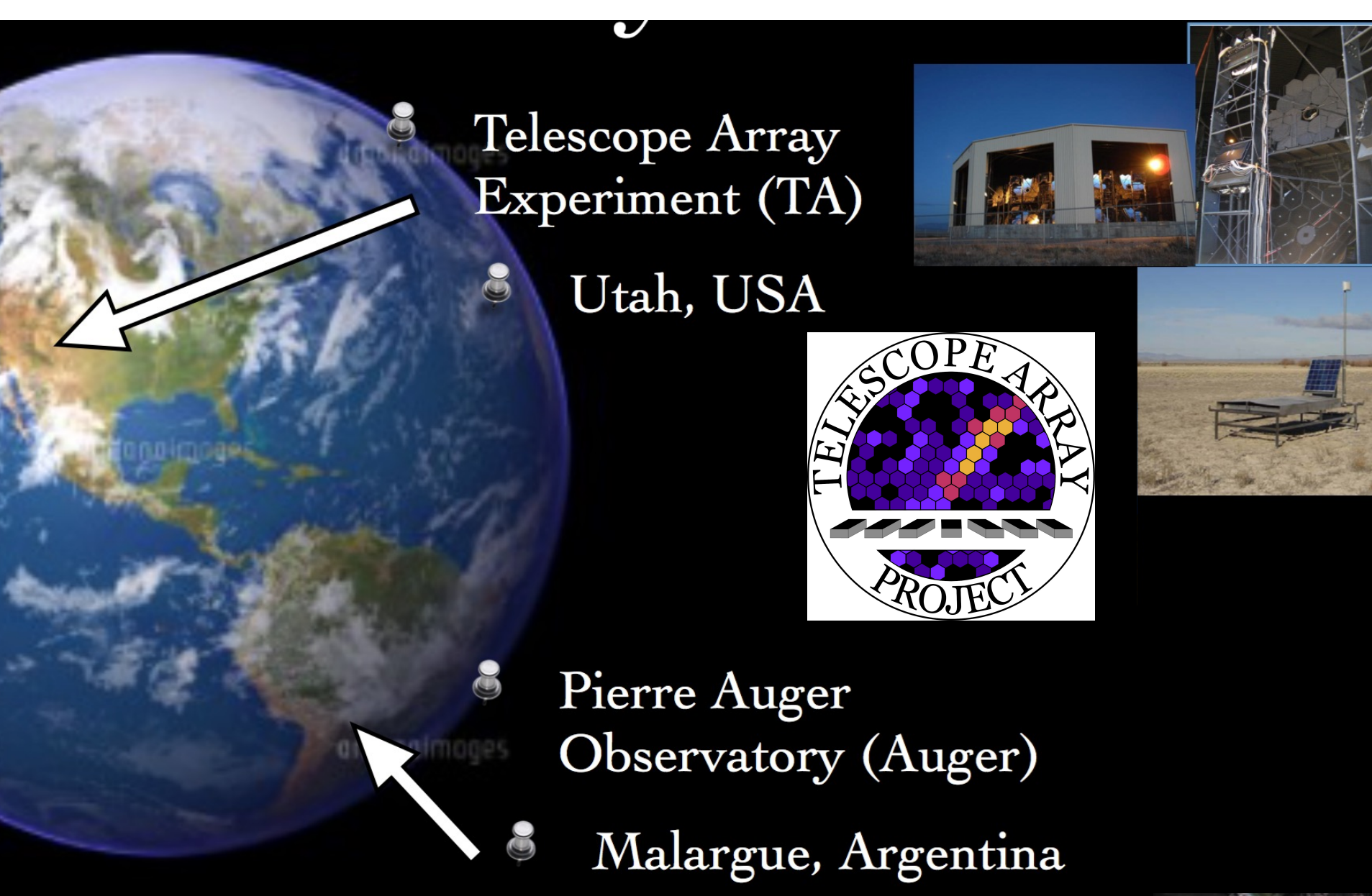
Plastic Scintillators such as **AMIGA** or **MuScint**



The Collaboration is working to chose the best solution in term of performances and cost.



The Telescope Array (TA)



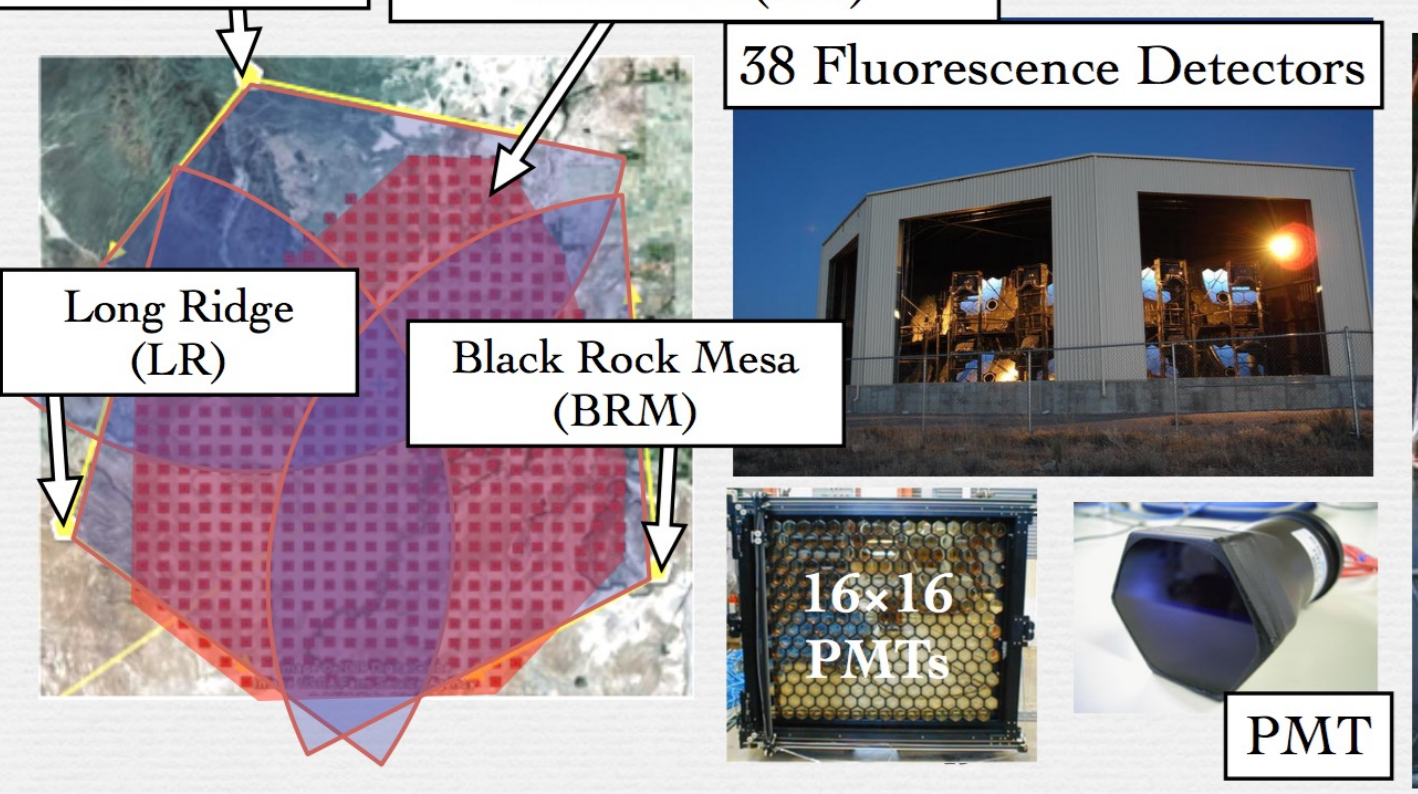


Telescope Array Experiment





- The largest detector in northern hemisphere: 700 km²
- Utah desert, US
- Hybrid detector using SDs and FDs
- Full operation from 2008
- Plastic Scintillator, sensitive to EM

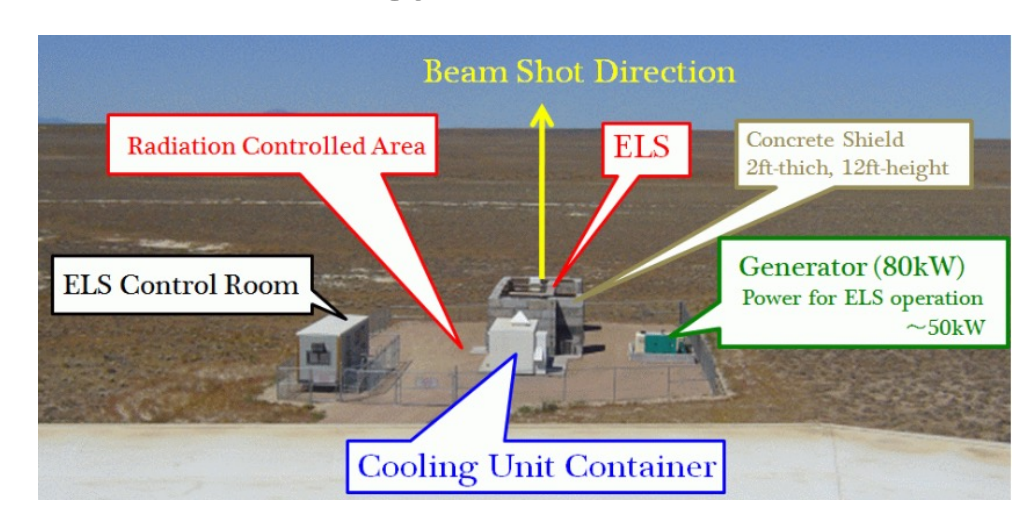




Electron Linear Accelerator (ELS) for Absolute energy calibration of the

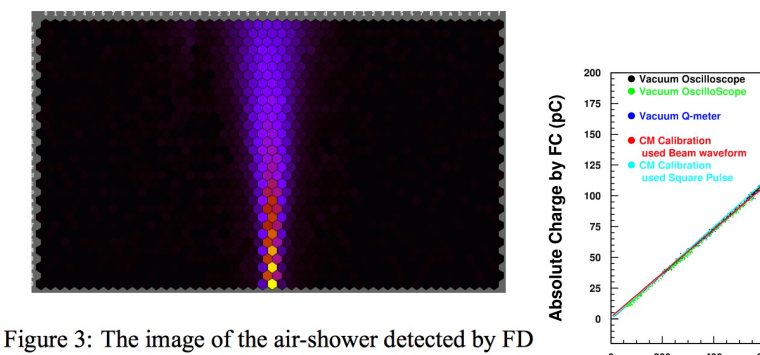
Telescope Array fluorescence detector

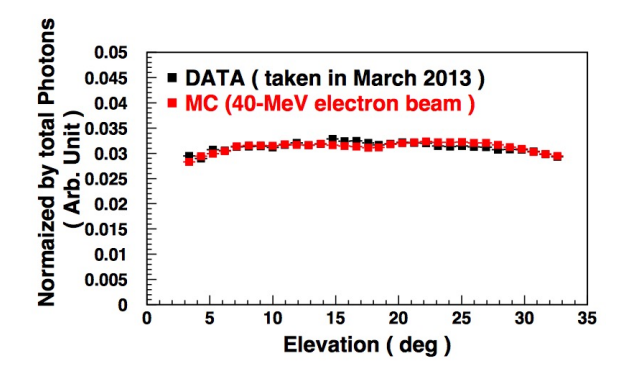
The Electron Light Source (ELS) is an electron linear accelerator, which was installed 100m in front of the Fluorescence Detector (FD) of Telescope Array (TA) experiment



Beam of **40 MeV electron**s is vertically injected into the air from the ELS and generated Air Fluorescence (AF) photons are detected by the TA/FD telescope.

A direct calibration of the TA/FD is achieved by comparing the measured ELS signal with the predicted signal by simulation using a model of AF generation.

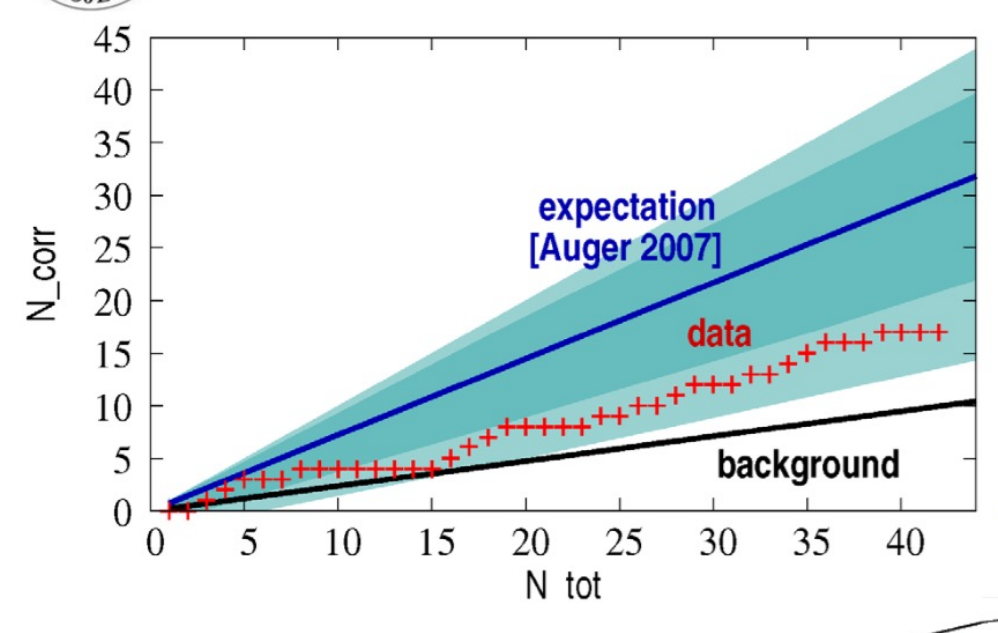




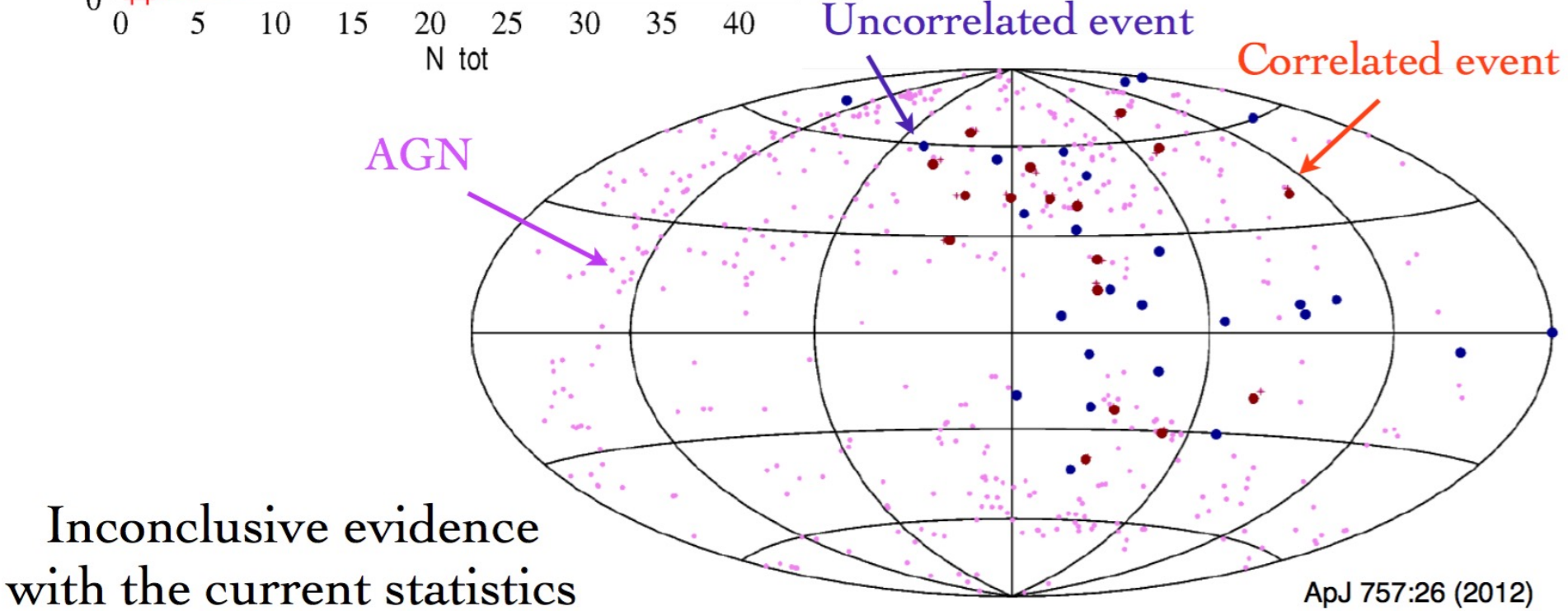
Core Monitor Output (mV*us)



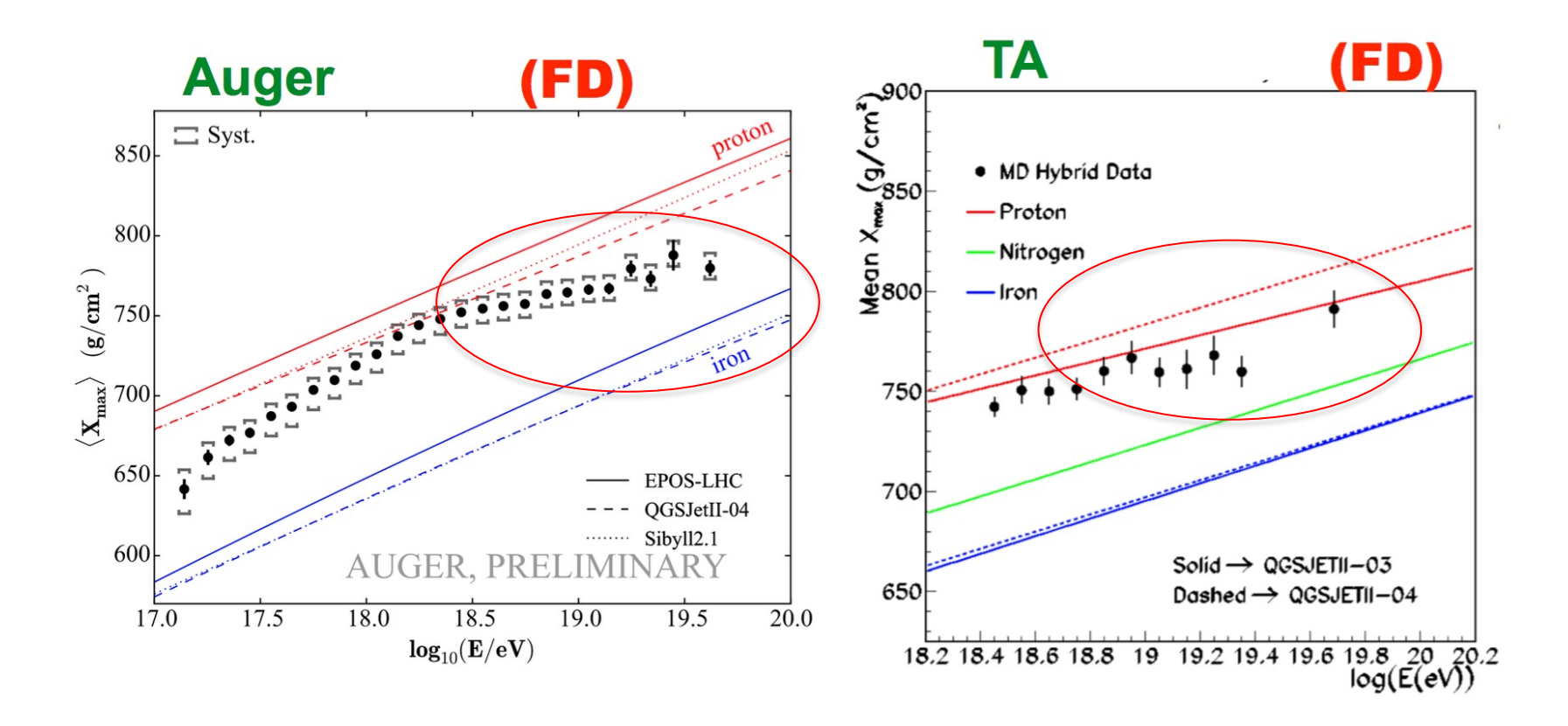
Correlation with Nearby AGN (TA)



3.1 degree circle
VCV catalog z < 0.018
(same condition with Auger)
E > 5.7×10¹⁹ eV in TA E-scale,
17 out of 42 events
(40%, P=0.014)



Tensione nei risultati di Auger e TA sulla composizione di massa alle **più alte energie**Mass Composition in <Xmax>

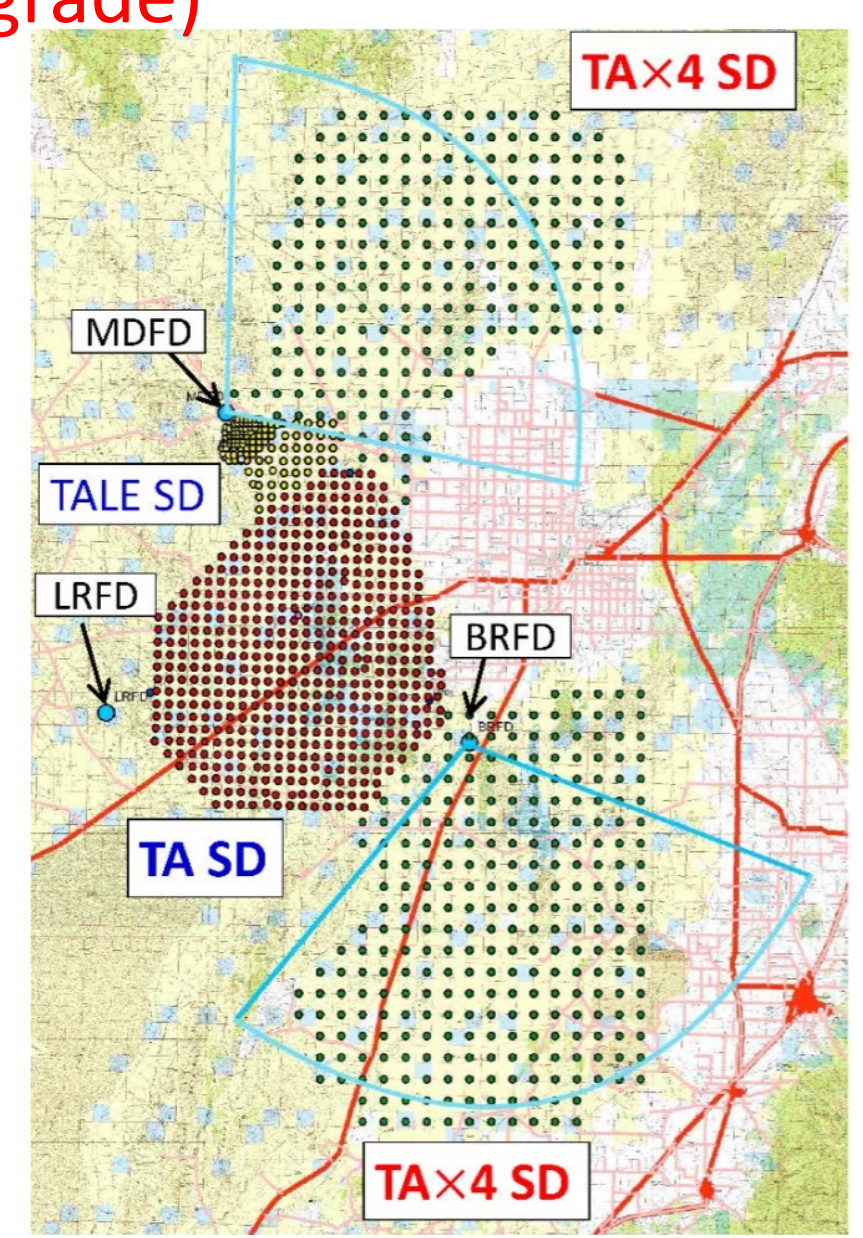


CAVEAT: Vengono utilizzati <u>differenti modelli di interazione adronica</u> e <u>differenti strategie di analisi</u>.

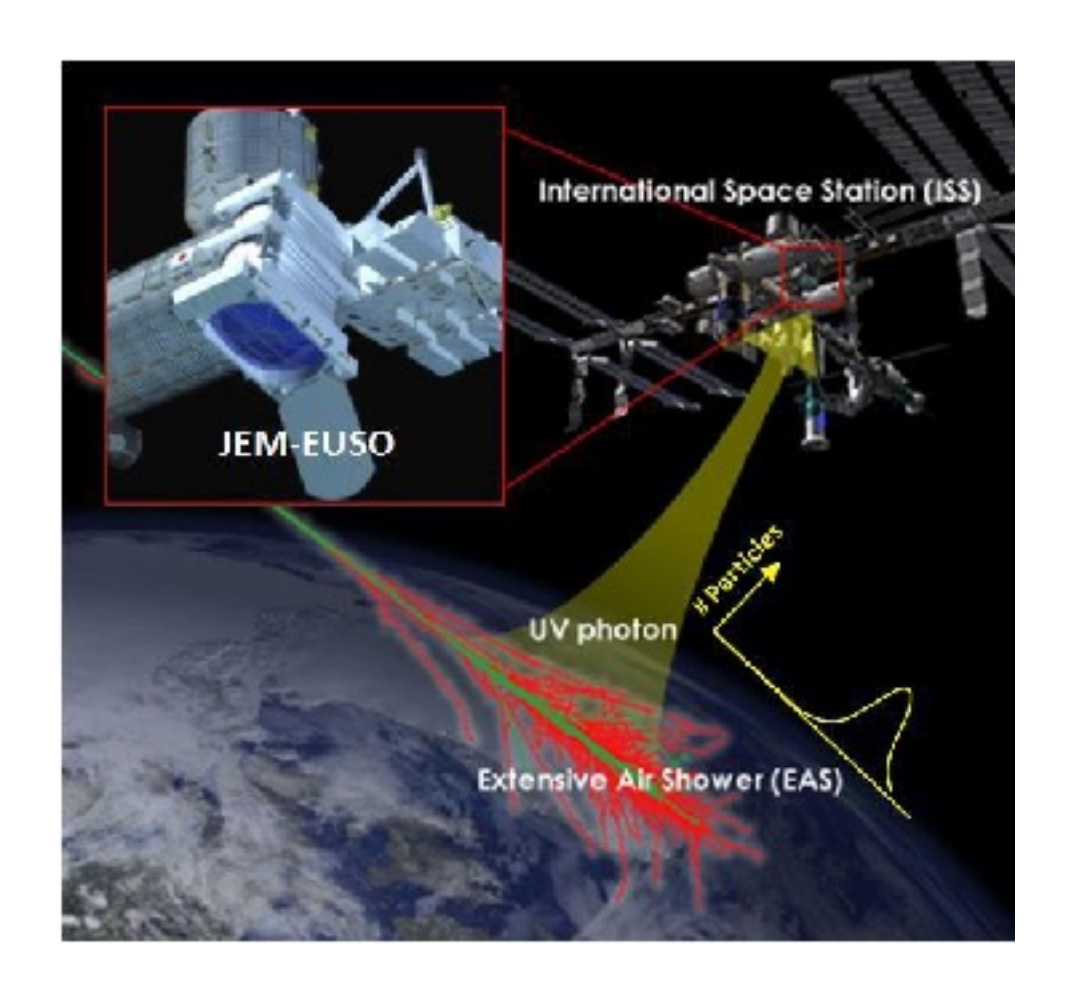
E' in corso un'analisi comune

TAUP (Telescope Array Upgrade)

- TAUP_{graded}.
- TAx4 = TA + TAx3, \sim 3000km²
- 500 SDs, 2km spacing
- 2 FD stations
- SD: Approved the proposal by Japan Apr. 2015
- FD: submitting proposal in
 US in Oct 2015

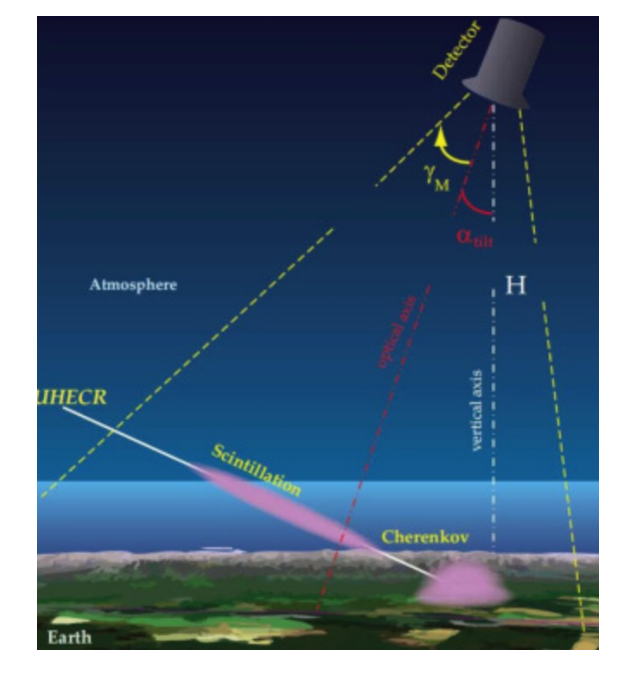


JEM-EUSO experiment, Extreme Universe Space Observatory on the International Space Station (ISS).



JEM-EUSO is, based on a UV telescope, which uses the **whole Earth as detector** from an altitude of ~ 400 km,

The fluorescence tracks is produced at (330-400) nm by Extensive Air Showers (EAS)



The launch is foreseen for the 2018 and the mission will last at least 5 years.

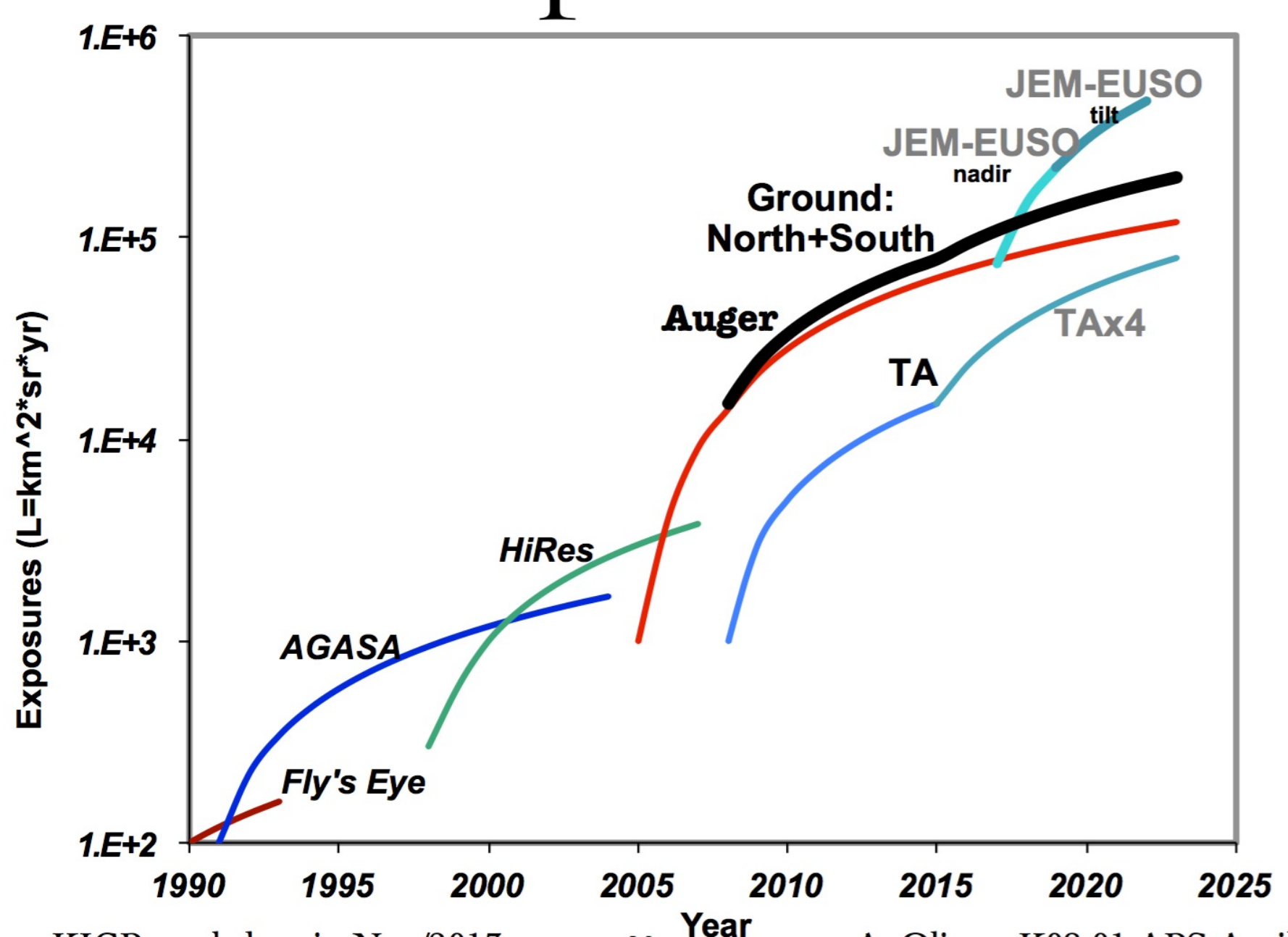
JEM-EUSO will be operated for three years in **Nadir configuration** to maximize statistics at the lowest energies in order to cross calibrate with the current generation of ground-based detectors.

The instrument will be then **tilted (about 30°)** with respect to Nadir in order to exploit a larger amount of atmosphere and to maximize the statistics of events at the highest energies.

The instantaneous aperture of JEM-EUSO is larger than that of successful Pierre Auger Observatory by a factor of 50 - 250

55

Exposure



La rivelazione degli EAS con radio onde

Cosmic-ray air showers emit radio waves in the frequency range few MHz – few 100 MHz. This effect opens many possibilities in the study of UHE and EHE extensive air showers.

There are **two effects** known which may <u>produce radio</u> <u>emission by cosmic ray showers</u>:

- 1) J.V. Jelley and H.R. Allan proposed the **radio emission** for air showers to be a **geomagnetic mechanism**.
- The coherent radio Cerenkov emission or Askaryan-Effect.

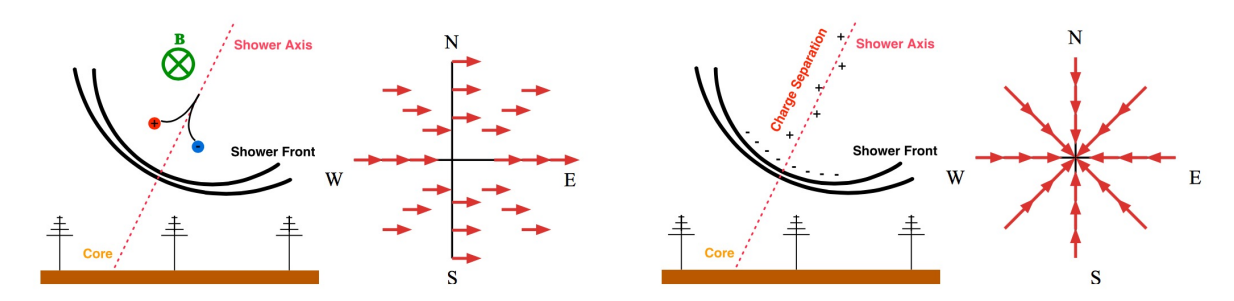


Figure 2: Schematic representation of the two main mechanisms contributing to the radio signal from extensive air showers.

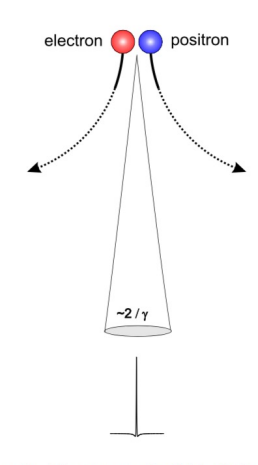


Figure 2: The magnetic field of the earth forces electrons and positrons on a counter circular movement creating radio emission with an opening angle $2/\gamma$

Fluorescence detectors with a calorimetric energy measurement allow to directly determine the depth of the air shower maximum -> mass-sensitive parameter, but they achieve duty cycles of only $\approx 10-15\%$.

Radio detection promises to directly probe the electromagnetic component of the air shower, energy measurement, sensitivity to X_{max} , and a duty cycle of $\approx 100\%$.

First-generation modern MHz experiments:

LOPES (LOfar PrototypE Station) and CODALEMA experiments measuring in the frequency range between the AM band at ~ 20 MHz and the FM band at ~ 80 MHz. Both experiments have access to energies of up to $\sim 10^{18}$ eV.

Second-generation modern MHz experiments:

the Auger Engineering Radio Array (AERA), the Tunka radio extension (Tunka-Rex), the Low Frequency Array (LOFAR).

AERA 3000 km² finanziamento 3.5 Meuro 2018



the frequency range from 30 to 80 MHz is investigated with **AERA**. **160 radio antennas** on an area of 20 km² to measure air showers with energies above **10**¹⁷ eV.

Radio emission from air showers in

Evidenza dell'origine extra-galattica degli UHECR

COSMIC RAYS

Science

Observation of a large-scale anisotropy in the arrival directions of cosmic rays above 8×10^{18} eV

The Pierre Auger Collaboration*+

Cosmic rays are atomic nuclei arriving from outer space that reach the highest energies observed in nature. Clues to their origin come from studying the distribution of their arrival directions. Using 3 \times 10⁴ cosmic rays with energies above 8 \times 10¹⁸ electron volts, recorded with the Pierre Auger Observatory from a total exposure of 76,800 km² sr year, we determined the existence of anisotropy in arrival directions. The anisotropy, detected at more than a 5.2 σ level of significance, can be described by a dipole with an amplitude of 6.5 $^{+1.3}_{-0.9}$ percent toward right ascension $\alpha_{\rm d}$ = 100 \pm 10 degrees and declination $\delta_{\rm d}$ = -24^{+12}_{-13} degrees. That direction indicates an extragalactic origin for these ultrahighenergy particles.

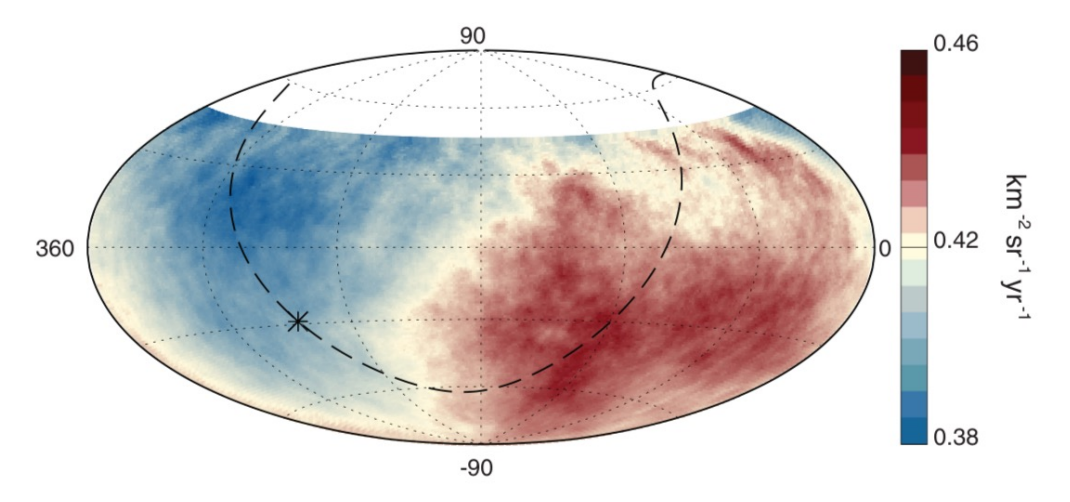


Fig. 2. Map showing the fluxes of particles in equatorial coordinates. Sky map in equatorial coordinates, using a Hammer projection, showing the cosmic-ray flux above 8 EeV smoothed with a 45° top-hat function. The galactic center is marked with an asterisk; the galactic plane is shown by a dashed line.

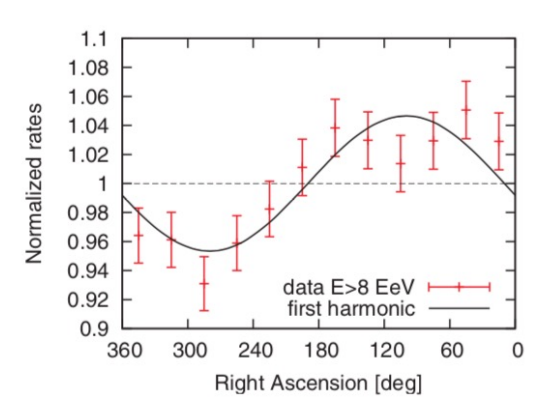


Fig. 1. Normalized rate of events as a function of right ascension. Normalized rate for 32,187 events with $E \ge 8$ EeV, as a function of right ascension (integrated in declination). Error bars are 1σ uncertainties. The solid line shows the first-harmonic modulation from Table 1, which displays good agreement with the data $(\chi^2/n = 10.5/10)$; the dashed line shows a constant function.

Table 1. First harmonic in right ascension. Data are from the Rayleigh analysis of the first harmonic in right ascension for the two energy bins.

Energy (EeV)	Number of events	Fourier coefficient a_{α}	Fourier coefficient b_{α}	Amplitude r_{lpha}	Phase φ _α (°)	Probability $P (\geq r_{\alpha})$
4 to 8	81,701	0.001 ± 0.005	0.005 ± 0.005	0.005 +0.006 -0.002	80 ± 60	0.60
≥8	32,187	-0.008 ± 0.008	0.046 ± 0.008	0.047 +0.008 -0.007	100 ± 10	2.6 × 10 ⁻⁸

Table 2. Three-dimensional dipole reconstruction. Directions of dipole components are shown in equatorial coordinates.

Energy (EeV)	Dipole component d _z	Dipole component d ₁	Dipole amplitude d	Dipole declination δ_d (°)	Dipole right ascension $a_{ m d}$ (°)
4 to 8	-0.024 ± 0.009	$0.006^{+0.007}_{-0.003}$	$0.025\substack{+0.010 \\ -0.007}$	-75 ⁺¹⁷	80 ± 60
≥8	-0.026 ± 0.015	$0.060^{+0.011}_{-0.010}$	$0.065^{+0.013}_{-0.009}$	-24 ⁺¹² ₋₁₃	100 ± 10

UHECRs & Hadronic Interactions

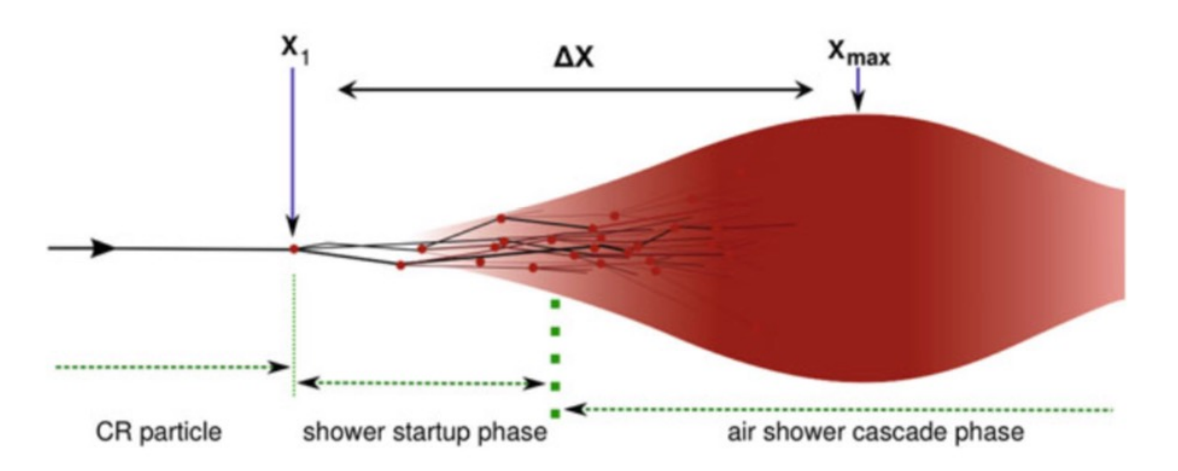
Cosmic rays at ultrahigh give a unique opportunity to study particle physics at energies well above those reachable at the LHC.

LHC UHECRs
14 TeV (cms) 400 TeV (cms)

X_{max} (expressed in g/cm²) may be defined as the sum of the

depth of the first interaction X_1 and a shower development length $\mathbb{Z}\Delta X$:

$$X_{\text{max}} = X_1 + \Delta X$$



$$\exp(-X_1/\Lambda_\eta)$$

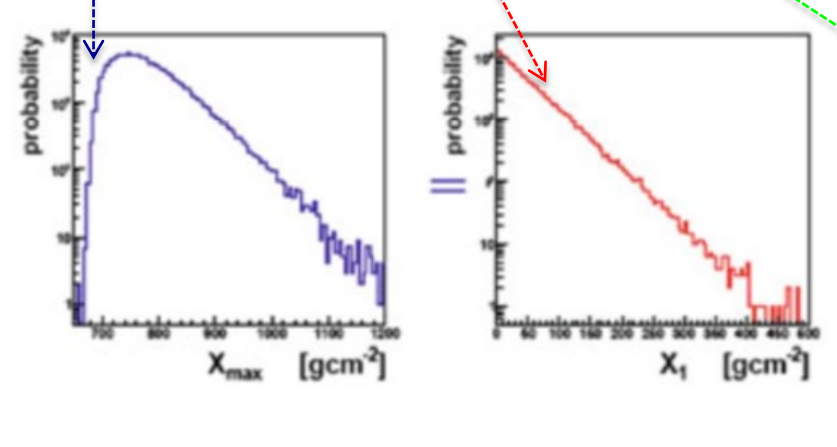
The X_1 distribution is just a negative exponential, $\exp(-X_1/\Lambda \mathbb{I}_{\eta})$, where $\Lambda_{\mathbb{I}\eta}$ is the interaction length which is proportional to the inverse of the cosmic ray—air interaction cross section.

60

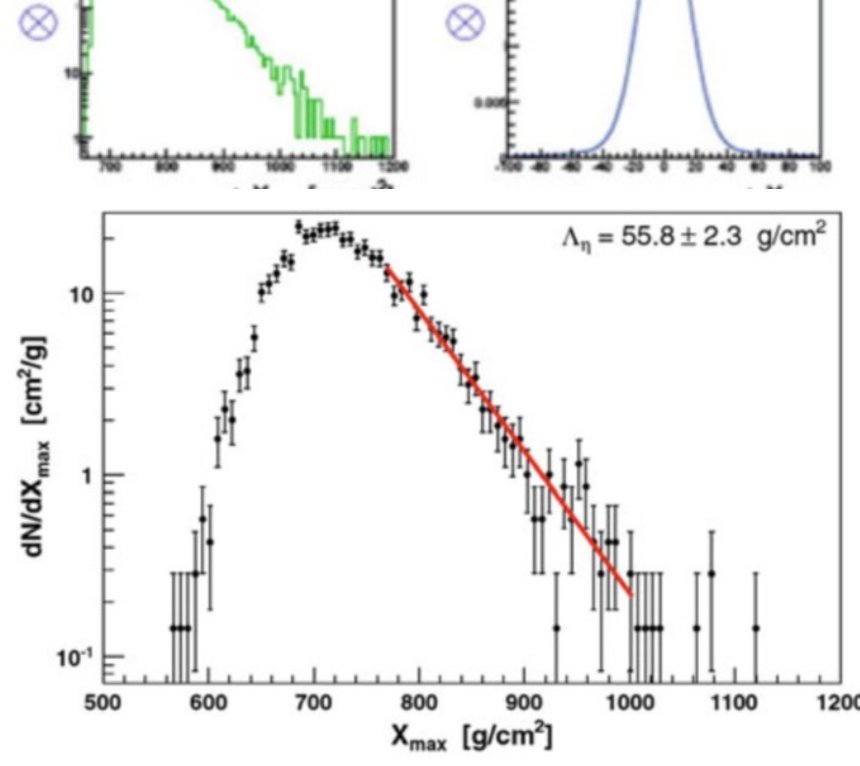
The **observed** X_{max} distribution is thus the **convolution** of the

- X₁ distribution with the
- Δ②X distribution (which has a shape similar to the X_{max} distribution) and a
- detector resolution function.

NB: the tail of the X_{max} distribution reflects the X_1 exponential distribution



 X_{max} distribution measured by the Pierre Auger Observatory in the energy interval 10^{18} – $10^{18.5}$ eV. The line represents the likelihood fit performed to extract Λ_n .



The conversion to proton—proton total and inelastic cross section is then done using the <u>Glauber model</u> which takes into account the multi-scattering probability inside the nuclei

Cross section proton-proton

